SRESA Journal of

Life Cycle Reliability and Safety Engineering

Vol. 1 I Issue No. 1 January – March 2012 ISSN – 2250 0820

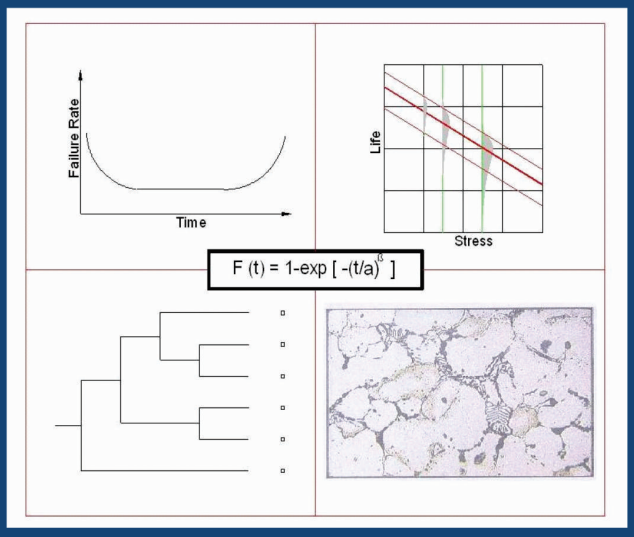

Chief-Editors:
P.V. Varde,
A.K. Verma
Michael G. Pecht

Society for Reliability and Safety

SRESA Journal of Life Cycle Reliability and Safety Engineering

Extensive work is being performed world over on assessment of Reliability and Safety for engineering systems in support of decisions. The increasing number of risk-based / risk-informed applications being developed world over is a testimony to the growth of this field. Here, along with probabilistic methods, deterministic methods including Physics-of-Failure based approach is playing an important role. The International Journal of Life Cycle Reliability and Safety Engineering provides a unique medium for researchers and academicians to contribute articles based on their R&D work, applied work and review work, in the area of Reliability, Safety and related fields. Articles based on technology development will also be published as Technical Notes. Review articles on Books published in the subject area of the journal will also form part of the publication.

Society for Reliability and Safety has been actively working for developing means and methods for improving system reliability. Publications of quarterly News Letters and this journal are some of the areas the society is vigorously pursuing for societal benefits. Manuscript in the subject areas can be communicated to the Chief Editors. Manuscript will be reviewed by the experts in the respective area of the work and comments will be communicated to the corresponding author. The reviewed final manuscript will be published and the author will be communicated the publication details. Instruction for preparing the manuscript has been given on inside page of the end cover page of each issue. The rights of publication rest with the Chief-Editors.

SCOPE OF JOURNAL

System Reliability analysis	**Structural Reliability**	**Risk-based applications**
Statistical tools and methods	Remaining life prediction	Technical specification optimization
Probabilistic Safety Assessment	Reliability based design	Risk-informed approach
Quantitative methods	Physics-of-Failure methods	Risk-based ISI
Human factor modeling	Probabilistic Fracture Mechanics	Risk-based maintenance
Common Cause Failure analysis	Passive system reliability	Risk-monitor
Life testing methods	Precursor event analysis	Prognostics & health management
Software reliability	Bayesian modeling	Severe accident management
Uncertainty modeling	Artificial intelligence in risk and reliability modeling	Risk-based Operator support systems
Dynamic reliability models	Design of Experiments	Role of risk-based approach in Regulatory reviews
Sensitivity analysis	Fuzzy approach in risk analysis	Advanced electronic systems reliability modeling
Decision support systems	Cognitive framework	Risk-informed asset management

SRESA AND ITS OBJECTIVES

a) To promote and develop the science of reliability and safety.

b) To encourage research in the area of reliability and safety engineering technology & allied fields.

c) To hold meetings for presentation and discussion of scientific and technical issues related to safety and reliability.

d) To evolve a unified standard code of practice in safety and reliability engineering for assurance of quality based professional engineering services.

e) To publish journals, books, reports and other information, alone or in collaboration with other organizations, and to disseminate information, knowledge and practice of ensuring quality services in the field of Reliability and Safety.

f) To organize reliability and safety engineering courses and / or services for any kind of energy systems like nuclear and thermal power plants, research reactors, other nuclear and radiation facilities, conventional process and chemical industries.

g) To co-operate with government agencies, educational institutions and research oganisations

SRESA Journal of

LIFE CYCLE RELIABILITY AND SAFETY ENGINEERING

Vol.1 Issue No.1 January – March 2012 ISSN – 2250 0820

Chief-Editors

P.V. Varde
A.K. Verma
Michael G. Pecht

SOCIETY FOR RELIABILITY AND SAFETY

Typeset & Printed

EBENEZER PRINTING HOUSE
Unit No. 5 & 11, 2nd Floor, Hind Services Industries,
Veer Savarkar Marg,
Dadar (west), Mumbai -28
Tel.: 2446 2632/ 3872
E-mail: outwork@gmail.com

Life Cycle Reliability and Safety Engineering
Vol.1 Issue 1 (2012) 01-14

Health Assessment of Three Dimensional Large Structural Systems – A Novel Approach

Ajoy Kumar Das[1] and Achintya Haldar[2*]

[1]*Doctoral Student, Dept. of Civil Engineering & Engineering Mechanics, University of Arizona, P.O. Box 210072, Tucson, AZ 85721, USA; PH +1 (520) 621-2266; FAX: (520) 621-2550; email: akdas@email.arizona.edu*

[2]*Professor, Dept. of Civil Engineering & Engineering Mechanics, University of Arizona, P.O. Box 210072, Tucson, AZ 85721, USA; PH +1 (520) 621-2142; FAX: (520) 621-2550; email: haldar@u.arizona.edu*

Abstract

A finite-elements-based time-domain system identification technique is presented in this paper for health assessment of three dimensional structures and denoted as 3D GILS-EKF-UI. It is a model-based procedure and represents structures by finite elements. The method integrates an iterative least-squares technique and the extended Kalman filter-based concept for detecting location(s) of defect(s) and their severity for the rapid assessment of structural health. It tracks the changes in stiffness parameters at the finite element level using dynamic response information. The procedure does not require information on dynamic excitation and uses noise-contaminated responses measured only at small part(s) of the structure. With the help of examples, it is demonstrated that the method is capable of accurately identifying defect-free and defective states of three dimensional structures. The method addresses several implementation issues for rapid, economical, and easier assessment of structural health. Considering the accuracy and robustness, it is expected that the procedure can be used as a vibration-based nondestructive health assessment procedure.

Keywords- *Finite elements; Time-domain; System identification; Unknown input excitation; Defects; Health assessment*

1. Introduction

Structural health assessment (SHA) of aging infrastructures has become one of the major challenges to the engineering community and attracted multidisciplinary worldwide research interest in the recent past. Lack of available resources to build new or replace old infrastructures prompted the researchers to develop alternatives to extend life of existing infrastructures. Most aged structures are expected to contain few defects; thus assessing their overall health as defective may not be of interest. Also, all defects are not equally important. It will be most advantageous if the defect(s) and their severity can be identified at the local element level. This will help to take appropriate remedial actions when necessary. With the availability of the advanced computational capabilities and sensor technologies, this alternative has become very attractive. The basic concept behind SHA has been under development by multidisciplinary research teams over the past several decades and a volume of information is already available in the existing literature. One can find a paper by Kerschen et al. (2006) with 446 references. Several state-of-the-art papers on civil engineering applications will also establish the extent of interest in the research communities (Lew et al., 1993; Ghanem and Shinozuka, 1995; Shinozuka and Ghanem, 1995; Doebling et al., 1996; Farrar and Doebling, 1997; Salawu, 1997; Carden and Fanning, 2004; Sohn et al., 2004; Kerschen et al., 2006; Humar et al., 2006; Nasrellah, 2009; Fan and Qiao, 2010). Several methods with various levels of sophistication are now available. It is not possible to identify them here and discuss their merits and demerits. However, they may not be directly applied to assess health of large structural systems, providing information on location(s), number, types of defects and their severity, thus limiting their application potential (Das et al, 2012). Considering accuracy,

efficiency, robustness, and economy, a new SHA technique is urgently needed and presented in this paper. It will provide an alternative to the commonly used subjective visual inspection-based SHA procedure. The ineffectiveness of visual inspections is extensively documented in the literature (Fritzen, 2006).

2. Necessity of a new SHA method

To develop a new SHA method using modern technology, some of its desirable features need to be identified first. It has been established in the profession that measuring the current dynamic responses of a structure as opposed to static responses is more attractive for the SHA purpose (Das et al., 2012). Limiting discussion on SHA using dynamic response information only, the new procedure can be developed in the frequency or time domain. Since frequency-domain modal properties represent global properties, it may not be efficient to locate defects at the local element level. This leads to the conclusion by the authors and their research team that a time-domain approach is necessary.

In locating defects at the local structural elements, i.e., in beams, columns, or other structural elements, an inverse transformation technique, commonly known as the system identification (SI) algorithm is widely used. In a typical SI-based algorithm, the three essential components are: (i) excitation(s) that will excite a structure to be identified, (ii) the structure, generally represented in an algorithmic form, i.e., in a finite elements (FEs) representation, and (iii) dynamic response information measured at different parts of the structure. Using information on the excitation and responses, the dynamic properties of the structure in terms of mass and stiffness properties of all the elements and damping can be identified. Assuming that the masses of all the elements can be estimated with sufficient accuracy and damping is applicable to the whole structure, the stiffness properties of all the elements can be tracked for the structural health assessment purpose. By comparing the identified stiffness properties with the expected values, or reference values obtained from the design drawings, or changes from the previous values if inspections are carried out periodically, or variations from one member to another with similar sectional properties, the location(s), number, and severity of defects can be established. The procedure should also be applicable to evaluate repaired structures indicating the effectiveness of the repairing process and whether all the defects are properly identified and repaired or not.

The basic concept behind SI-based SHA methods appears to be straight forward. Some of the basic questions generally raised are on how to establish the uniqueness of the identified parameters and the convergence criteria. Assuming at this time that the numerical aspects of the SI-based formulation can be adequately addressed, the question remains is whether it can be successfully implemented to assess health of large structural systems. The implementation issues were generally overlooked in the past. To incorporate implementation issues appropriately, the basic SI-based SHA concept will need significant modifications or improvements. The improvements, as discussed next, will provide a platform for a novel concept.

Measuring excitation information accurately is a major challenge even in the controlled laboratory environment. It will be a major challenge if excitation information needs to be measured for real existing structures in field conditions. Therefore, it will be highly desirable if a system can be identified using only measured response information, completely ignoring the excitation information. However, it will be mathematically challenging since two of the three basic components of SI algorithm will be unknown. Several implementation issues also need to be appropriately addressed in the novel SHA procedure. First, considering the advance nature of current sensor technology, the most appropriate sensor for measuring dynamic responses in time-domain will be smart accelerometers with very high sampling rate. However, the acceleration time-histories, even when measured by smart accelerometers, are expected to be noise contaminated. The presence of noise in the measured responses requires special attention. Second, a large number of

dynamic degrees of freedom (DDOFs) will be necessary to represent large structural systems. It will be practically impossible and economically infeasible to instrument sensors at all DDOFs of large systems. Response information may be available only at a small part(s) of the structure where sensors are placed. The above discussions suggest that a novel time-domain SI-based SHA technique needs to be developed that can identify large structure systems, represented by finite elements, using only limited noise-contaminated response information measured at small part(s) of the structure and completely ignoring the excitation information.

The research team at the University of Arizona has been working on developing such a novel approach. The method can be economically implemented with relative ease for rapid diagnostic of the health of a structure. The implementation of the approach for assessing health of large three dimensional (3D) structures is specifically addressed in this paper.

3. Mathematical Formulation

Identification of large structural systems with limited measured response information will necessitate the use of a substructure concept. Based on the locations of sensors, a substructure can be defined first. It will then be necessary to identify the substructure completely ignoring the excitation information, as suggested by Wang and Haldar (1994). The extended Kalman filter (EKF)-based algorithm is generally used when the response information is limited and noise contaminated (Wang and Haldar, 1997). The structural responses can be nonlinear due to presence of large deformation, defects, or high level of excitation. To incorporate a moderate level of nonlinearity, the EKF can be used by modeling structural behavior as piece-wise linear. The use of EKF will also help to incorporate error in the basic mathematical model representing the structure as well as the presence of noise in the response information. However, there are two fundamental obstructions of use of EKF in structural identification. To satisfy the dynamic governing equations even for the substructure, the excitation information must be known. However, it is considered to be unknown at this stage, thus defeating one of the main desirable features of the novel approach. Also, the initial state vector of the whole structure must be known, but it is unknown at this stage; it is supposed to be the outcomes of the identification process to assess structural health. The discussions clearly indicate that the basic EKF-based method available in the literature cannot be used; the information required to implement it must be intelligently generated.

To meet the basic objective of a novel SHA technique, the research team proposed a two-stage approach. In stage 1, the substructure discussed earlier will be identified without using excitation information by using a procedure already developed by the team (Katkhuda and Haldar, 2008). When Stage 1 is implemented properly, it will generate excitation information. This will satisfy one of the two basic obstructions to implement the EKF concept. Also, the identified stiffness properties of all the elements in the substructure, if used judicially, can provide information on the initial state vector, as will be discussed later in detail. This will satisfy the second basic obstruction to implement the EKF concept. With the generated information on the unknown time history of excitation and the initial state vector in Stage 1, the stiffness parameters for the whole structure can be identified using the EKF concept in Stage 2. By combining Stages 1 and 2, a novel SHA method will be developed. It will be denoted hereafter as the 3D Generalized Iterative Least-Squares Extended Kalman Filter with Unknown Input method or 3D GILS-EKF-UI. As discussed earlier, the identified stiffness parameters of all the structural elements can be used to assess the structural health. The mathematical concepts behind these two stages are discussed very briefly next.

Health assessment of three dimensional structures: Stage 1 – Concept of 3D GILS-UI

Without losing the generality, suppose the health of a three dimensional structure shown in Figure 1 needs to be assessed. However, the response information is measured only at node 1, 2, 3, and 5. The task is to identify the health of

the whole structure using only limited response information available in the substructure.

Based on the available response information, the required substructure in Stage 1 can be selected as shown with double lines in Figure 1. The whole structure consists of 12 beams and 12 columns. The substructure consists of two beams and one column. From the implementation point of view, it is expected that the point of application of the excitation and measured responses at node points will be close to each other. To set up the inspection process, it is necessary that the unknown exciting force will be applied at a node in the substructure.

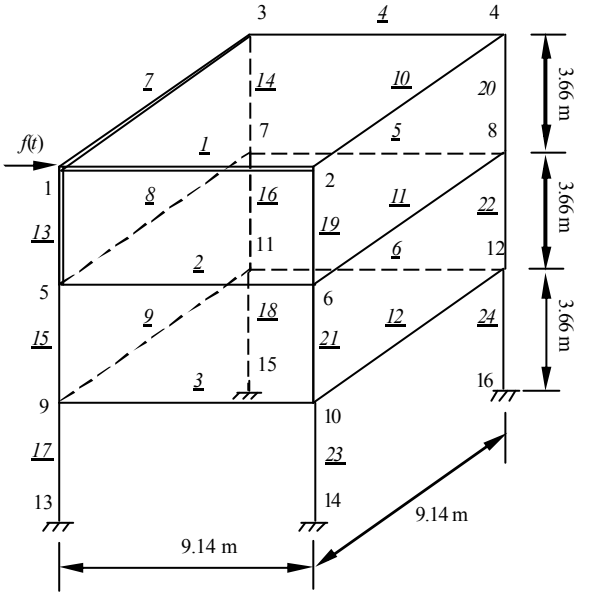

Figure 1. FE representation of a three dimensional frame

The governing differential equation of motion using Rayleigh damping for the substructure can be expressed as (Ling and Haldar, 2004):

$$\mathbf{M}_{sub}\ddot{\mathbf{X}}_{sub}(t) + (\alpha\mathbf{M}_{sub}+\beta\mathbf{K}_{sub})\dot{\mathbf{X}}_{sub}(t) + \mathbf{K}_{sub}\mathbf{X}_{sub}(t) = \mathbf{f}_{sub}(t) \quad (1)$$

where $\mathbf{M}_{sub}$ is the global mass matrix; $\mathbf{K}_{sub}$ is the global stiffness matrix; $\ddot{\mathbf{X}}_{sub}(t)$, $\dot{\mathbf{X}}_{sub}(t)$, and $\mathbf{X}_{sub}(t)$ are the vectors containing the acceleration, velocity, and displacement, respectively, at time t; $\mathbf{f}_{sub}(t)$ is the input excitation vector at time t; and α and β are the mass and stiffness proportional Rayleigh damping coefficients, respectively. The subscript 'sub' is used to denote substructure.

For a typical 3D frame element, the mass matrix $\mathbf{M}_i$ and stiffness matrix $\mathbf{K}_i$ of the ith member, in the local coordinate system are expressed as (Paz, 1985):

$$\mathbf{M}_i = \frac{\bar{m}_i L_i}{420}\begin{bmatrix} 140 & 0 & 0 & 0 & 0 & 0 & 70 & 0 & 0 & 0 & 0 & 0 \\ 0 & 156 & 0 & 0 & 0 & 22L_i & 0 & 54 & 0 & 0 & 0 & -13L_i \\ 0 & 0 & 156 & 0 & -22L_i & 0 & 0 & 0 & 54 & 0 & 13L_i & 0 \\ 0 & 0 & 0 & 140c_i & 0 & 0 & 0 & 0 & 0 & 70c_i & 0 & 0 \\ 0 & 0 & -22L_i & 0 & 4L_i^2 & 0 & 0 & 0 & -13L_i & 0 & -3L_i^2 & 0 \\ 0 & 22L_i & 0 & 0 & 0 & 4L_i^2 & 0 & 13L_i & 0 & 0 & 0 & -3L_i^2 \\ 70 & 0 & 0 & 0 & 0 & 0 & 140 & 0 & 0 & 0 & 0 & 0 \\ 0 & 54 & 0 & 0 & 0 & 13L_i & 0 & 156 & 0 & 0 & 0 & -22L_i \\ 0 & 0 & 54 & 0 & -13L_i & 0 & 0 & 0 & 156 & 0 & 22L_i & 0 \\ 0 & 0 & 0 & 70c_i & 0 & 0 & 0 & 0 & 0 & 140c_i & 0 & 0 \\ 0 & 0 & 13L_i & 0 & -3L_i^2 & 0 & 0 & 0 & 22L_i & 0 & 4L_i^2 & 0 \\ 0 & -13L_i & 0 & 0 & 0 & -3L_i^2 & 0 & -22L_i & 0 & 0 & 0 & 4L_i^2 \end{bmatrix} \quad (2)$$

and

$$\mathbf{K}_i = \frac{E_i I_{z_i}}{L_i}\begin{bmatrix} \frac{A_i}{I_{z_i}} & 0 & 0 & 0 & 0 & 0 & -\frac{A_i}{I_{z_i}} & 0 & 0 & 0 & 0 & 0 \\ 0 & \frac{12}{L_i^2} & 0 & 0 & 0 & \frac{6}{L_i} & 0 & -\frac{12}{L_i^2} & 0 & 0 & 0 & \frac{6}{L_i} \\ 0 & 0 & \frac{12}{L_i^2}a_i & 0 & -\frac{6}{L_i}a_i & 0 & 0 & 0 & -\frac{12}{L_i^2}a_i & 0 & -\frac{6}{L_i}a_i & 0 \\ 0 & 0 & 0 & b_i & 0 & 0 & 0 & 0 & 0 & -b_i & 0 & 0 \\ 0 & 0 & -\frac{6}{L_i}a_i & 0 & 4a_i & 0 & 0 & 0 & \frac{6}{L_i}a_i & 0 & 2a_i & 0 \\ 0 & \frac{6}{L_i} & 0 & 0 & 0 & 4 & 0 & -\frac{6}{L_i} & 0 & 0 & 0 & 2 \\ -\frac{A_i}{I_{z_i}} & 0 & 0 & 0 & 0 & 0 & \frac{A_i}{I_{z_i}} & 0 & 0 & 0 & 0 & 0 \\ 0 & -\frac{12}{L_i^2} & 0 & 0 & 0 & -\frac{6}{L_i} & 0 & \frac{12}{L_i^2} & 0 & 0 & 0 & -\frac{6}{L_i} \\ 0 & 0 & -\frac{12}{L_i^2}a_i & 0 & \frac{6}{L_i}a_i & 0 & 0 & 0 & \frac{12}{L_i^2}a_i & 0 & \frac{6}{L_i}a_i & 0 \\ 0 & 0 & 0 & -b_i & 0 & 0 & 0 & 0 & 0 & b_i & 0 & 0 \\ 0 & 0 & -\frac{6}{L_i}a_i & 0 & 2a_i & 0 & 0 & 0 & \frac{6}{L_i}a_i & 0 & 4a_i & 0 \\ 0 & \frac{6}{L_i} & 0 & 0 & 0 & 2 & 0 & -\frac{6}{L_i} & 0 & 0 & 0 & 4 \end{bmatrix} \quad (3)$$

where L_i, A_i, E_i, and $\bar{m}_i$ are the length, cross-section area, material Young's modulus of elasticity, and mass per unit length, respectively, of the ith frame element; and c_i, a_i, and b_i are defined as:

$$c_i = I_{\bar{m}_i} / \bar{m}_i \quad a_i = I_{y_i} / I_{z_i} \quad b_i = J_i / \left[2(1+\upsilon) I_{z_i} \right] \quad (4)$$

where I_{zi} and I_{yi} are the cross-sectional moment of inertias with respect to the major and minor principal axes, respectively; J_i is the torsional moment of inertia; υ is the Poisson's ratio of the material, and $I_{\bar{m}_i}$ is the polar mass moment of inertia per unit length of the member. Denoting the coefficient matrix in the square bracket by S_i, Eq. 3 can be written as $\mathbf{K}_i = k_i S_i$, where $k_i = E_i I_{zi} / L_i$, is defined as the stiffness parameter for the ith member. Matrices $\mathbf{M}_i$ and $\mathbf{K}_i$ in the element local coordinate system need to

be transformed to the global coordinate system using appropriate transformation matrix $\mathbf{T}_i$ to obtain the global mass and stiffness matrices, $\bar{\mathbf{M}}_i$ and $\bar{\mathbf{K}}_i$, as (Paz, 1985):

$$\bar{\mathbf{M}}_i = \mathbf{T}_i^T \mathbf{M}_i \mathbf{T}_i \quad \bar{\mathbf{K}}_i = k_i \mathbf{T}_i^T \mathbf{S}_i \mathbf{T}_i = k_i \bar{\mathbf{S}}_i \tag{5}$$

Considering all the elements in the substructure and using Eq. 5, the global mass and stiffness matrices for the substructure can be formulated as:

where *nesub* is the total number of elements

$$\mathbf{M}_{sub} = \sum_{i=1}^{nesub} \bar{\mathbf{M}}_i \tag{6}$$

$$\mathbf{K}_{sub} = \sum_{i=1}^{nesub} \bar{\mathbf{K}}_i = \sum_{i=1}^{nesub} k_i \bar{\mathbf{S}}_i \tag{7}$$

in the substructure. Using Eq. 7, Eq. 1 can be reorganized as:

$$\mathbf{f}_{sub}(t) - \mathbf{M}_{sub}\ddot{\mathbf{X}}_{sub}(t) = (k_1\bar{\mathbf{S}}_1 + k_2\bar{\mathbf{S}}_2 + \cdots + k_{nesub}\bar{\mathbf{S}}_{nesub})\mathbf{X}_{sub}(t)$$
$$+ \beta(k_1\bar{\mathbf{S}}_1 + k_2\bar{\mathbf{S}}_2 + \cdots + k_{nesub}\bar{\mathbf{S}}_{nesub})\dot{\mathbf{X}}_{sub}(t) + \alpha\mathbf{M}_{sub}\dot{\mathbf{X}}_{sub}(t) \tag{8}$$

Equivalently,

$$\mathbf{f}_{sub}(t) - \mathbf{M}_{sub}\ddot{\mathbf{X}}_{sub}(t) =$$
$$[\bar{\mathbf{S}}_1\mathbf{X}_{sub}(t)\ \bar{\mathbf{S}}_2\mathbf{X}_{sub}(t)\ \cdots\ \bar{\mathbf{S}}_{nesub}\dot{\mathbf{X}}_{sub}(t)\ \bar{\mathbf{S}}_1\dot{\mathbf{X}}_{sub}(t)\ \bar{\mathbf{S}}_2\dot{\mathbf{X}}_{sub}(t)\ \cdots$$
$$\cdots\ \bar{\mathbf{S}}_{nesub}\dot{\mathbf{X}}_{sub}(t)\ \mathbf{M}_{sub}\dot{\mathbf{X}}_{sub}(t)]\mathbf{P} \tag{9}$$

In the above equation, **P** is defined as follows:

$$\mathbf{P} = [k_1\ k_2\ \cdots\ k_{nesub}\ \beta k_1\ \beta k_2\ \cdots\ \beta k_{nesub}\ \alpha]^T$$

It contains unknown stiffness and damping parameters. Obviously, to solve for P, at least *Lsub = 2 nesub + 1* number of equations must be formed. As mentioned earlier, acceleration time histories will be measured at high sampling rates, i.e., the responses will be available at large number of time points. This will create a situation where the number of equations will be larger than required, indicating an over-determined system of equations. Using the error minimization technique, a least squares technique is formulated and used to solve these equations as discussed below.

Considering that the responses at all n time points are available, the Eq. 9 can be reorganized with N_{dkey}×n number of equations for the key node(s) (Katkhuda and Haldar, 2008) as:

$$\mathbf{F}_{Ndkey.n\times 1} = \mathbf{A}_{Ndkey.n\times Lsub}\mathbf{P}_{Lsub\times 1} \tag{10}$$

where N_{dkey} is the number of DDOFs for the key node(s) in the substructure. Vector F on the left hand side of Eq. 10 contains the unknown input excitations and the inertia forces at all n time points. Matrix A on the right hand side contains the measured displacement and velocity responses at all n time points. To implement the least-squares minimization technique, an error function (ε) is defined as:

$$\varepsilon = \sum_{r=1}^{Ndkey.n}\left(F_r - \sum_{s=1}^{Lsub} A_{rs}P_s\right)^2 \tag{11}$$

To satisfy the necessary condition for ε to be the minimum, the derivative of the error function with respect to vector **P** must be equated to zero, that is

$$\frac{d\varepsilon}{d\mathbf{P}} = 0 \tag{12}$$

Equation 12 leads to the least-square estimator given by

$$\mathbf{P}_{Lsub\times 1} = (\mathbf{A}^T_{Lsub\times Ndkeyn}\mathbf{A}_{Ndkeyn\times Lsub})^{-1}\mathbf{A}^T_{Lsub\times Ndkeyn}\mathbf{F}_{Ndkeyn\times 1} \tag{13}$$

It is relatively simple to solve for **P** using Eq. 13 provided the vector **F** is known. However, since the information on input excitations is not known, **F** becomes partially known. To start the iteration process using the least-squares technique, the excitation information was initially assumed to be zero for few time points as discussed by Wang and Haldar (1994). Katkhuda et al. (2005) implemented the iterative procedure by assuming the excitation information to be zero for all the time points. The iteration process is continued until the excitation time history converges at all time points, considering two successive iterations, with a predetermined tolerance

level. It is important to note that acceleration time histories will be measured during an inspection. To evaluate **P**, the corresponding velocity and displacement time histories are necessary. The acceleration time histories can be successively integrated to generate the velocity and displacement time histories as discussed in more detail by Vo and Haldar (2003). The concept has been extensively verified, analytically and experimentally, for two dimensional structures. For three dimensional structures discussed in this paper, the 3D GILS-UI procedure can be implemented using the following steps.

Steps to identify substructure in Stage 1 - 3D GILS-UI

Step 1 – Generate velocity and displacement time histories from measured acceleration time histories.

Step 2 - Form the *Ndkey* × *Lsub* matrix $A(t_k)$ in Eq. 9 for all discrete time steps t_k, for k = 1, 2, …, n, using the available dynamic responses in terms of velocities and displacements. Form the (Ndkey.n) × Lsub matrix A by appending all the $A(t_k)$ matrices, i.e.,

$$\mathbf{A}_{Ndkey.n\times Lsub} = [\mathbf{A}_{Ndkey\times Lsub}(t_1) \quad \mathbf{A}_{Ndkey\times Lsub}(t_2) \quad \cdots \quad \mathbf{A}_{Ndkey\times Lsub}(t_n)]^T \tag{15}$$

Step 3 - Assume that the Ndkey×1 input excitation force vectors $\mathbf{f}(t_k)$ to be zero for all the time steps, i.e., $f(t_k) = 0$, for k = 1, 2, ..., n. Form the (Ndkey.n) × 1 vector **f** by appending all the $\mathbf{f}(t_k)$ vectors. Using matrix **A** and force vector **F** obtain the first estimation of Lsub × 1 system parameter vector **P** using Eq. 13.

Step 4 - Substitute the system parameters **P** estimated in step 3 into Eq. 1 to obtain unknown input force vector **f**.

Step 5 - Apply force constraints to the input excitation **f** obtained in step 4. For example, if the input excitation is known to be exactly zero at j^{th} DDOF, the constraint $\mathbf{f}_j(t_k) = 0$, where k = 1, 2, …, n, needs to be introduced.

Step 6 - Obtain the updated information on the system parameter vector **P** using step 3.

Step 7 - Update the input excitation force vector **f** using Eq. 1 and then update the system parameter vector **P** again.

Continue the iteration procedure until a predetermined convergence tolerance level (d) on the input excitation is satisfied i.e. $\mathbf{f}^{i+1} - \mathbf{f}^i \le \delta$, where $\mathbf{f}^{i+1}$ and $\mathbf{f}^i$ are the excitation forces estimated in two consecutive iterations for all n time steps. A convergence tolerance level of 10^{-6} is considered for this study.

3D GILS-EKF-UI – Stage 2

As mentioned earlier, information generated in Stage 1 can be used to implement Stage 2 and the stiffness parameter of all the elements in the structural system can be evaluated. The EKF concept is relatively new and may not be known to all the readers. A brief discussion is made below to introduce the basic EKF concept for the readers who are not familiar with it.

Concept of EKF-WGI procedure

In order to implement the EKF concept, it is necessary to describe the dynamic system by a set of nonlinear differential equations. In the absence of any process noise, i.e., assuming the governing differential equation of motion Equation 1 is correct, expressing it in the state-space form will result a set of first-order nonlinear differential equation (Saridis, 1995) as:

$$\dot{\mathbf{Z}}(t) = f(\mathbf{Z}(t), t) \tag{16}$$

where f(**Z**(t),t) is the nonlinear function of the states and **Z**(t) can be mathematically expressed as:

$$\mathbf{Z}(t) = \begin{bmatrix} \mathbf{Z}_s(t) \\ \mathbf{Z}_p(t) \end{bmatrix} = \begin{bmatrix} \mathbf{X}(t) \\ \dot{\mathbf{X}}(t) \\ \tilde{\mathbf{K}} \end{bmatrix} \tag{17}$$

where the subscript s denotes the components of the system state vector and p denotes the system parameter vector to be identified. The vectors $\mathbf{X}(t)$ and $\dot{\mathbf{X}}(t)$ contain displacement and velocity responses of the system, respectively, and vector $\tilde{\mathbf{K}}$ contains the unknown system parameters assumed to remain invariant during the identification process.

For a structure consisting of ne numbers of elements, $\tilde{\mathbf{K}}$ can be defined as $\tilde{\mathbf{K}} = [k_2 \quad k_2 \quad \ldots \quad k_{ne}]^T$, where k_i is the stiffness parameter of the ith element. Equation 17 can be rewritten as:

$$\dot{\mathbf{Z}}(t) = \begin{bmatrix} \dot{\mathbf{X}}(t) \\ \ddot{\mathbf{X}}(t) \\ 0 \end{bmatrix} = \begin{bmatrix} \dot{\mathbf{X}}(t) \\ \mathbf{M}^{-1}\left[\mathbf{f}(t) - \alpha\mathbf{M}\dot{\mathbf{X}}(t) - \beta\mathbf{K}\dot{\mathbf{X}}(t) - \mathbf{K}\mathbf{X}(t)\right] \\ 0 \end{bmatrix} \quad (18)$$

Equation 16 is essentially a compact representation of Eq. 18.

Displacements and velocities are considered to be available at a constant time interval of Δt, at a discrete time instances $t_k = k\,\Delta t$ for a total duration of, say, T seconds. The discrete time measurement equation **Y**(k) is linear and noise contaminated, and it can be expressed at any discrete time k as:

$$\mathbf{Y}(k) = \mathbf{H} \cdot \mathbf{Z}(k) + \mathbf{V}(k) \quad (19)$$

where **H** is the measurement matrix; for measured responses it becomes a unit diagonal matrix, and **V**(k) is a zero-mean Gaussian white random process indicating the presence of noise. It is generally presented as:

$$\mathbf{V}(k) \sim N(0, \mathbf{R}(k)) \quad (20)$$

where **R**(k) is the discrete measurement noise matrix consisting of covariance values considering noise source in each measurement at any discrete time k. The noise covariance matrix is generally assumed to be diagonal and the values remain constant with time. In this study it is assumed to be of the same magnitude of 10^{-4} for all responses.

As mentioned earlier, before staring the filtering algorithm, it is necessary to have initial estimate of the uncertain state vector containing information of stiffness parameters of all the elements in the structure. It can be developed from the information generated in Stage 1. Suppose, the substructure contains a beam and a column and their stiffness parameters are identified in Stage 1. To develop the initial estimate of the state vector, all the beams in the structure will be assigned the same stiffness parameter value as obtained for the beam in the substructure. For columns, similar procedure will be followed. This is expected to be very reasonable since all the beams and all columns in the structure are expected to have respective similar stiffness parameters. This may help to accelerate the convergence process of their estimates.

To start the filtering process, the initial as well as the subsequent estimates of the state vector are considered to be uncertain and generally modeled as a Gaussian. Considering the initial state vector as represented as $\mathbf{Z}(0|0)$, it can be expressed as:

$$\mathbf{Z}(0|0) = (\hat{\mathbf{Z}}(0|0), \mathbf{P}(0|0)) \quad (21)$$

where $\hat{\mathbf{Z}}(0|0)$ is a vector containing the mean values. Since the initial values of the responses in the state vector are not available, they can be assumed to be zero. The initial values for the stiffness parameters, as discussed above, are assigned by judiciously using the values obtained in stage 1. Thus the initial state vector is exressed as:

$$\hat{\mathbf{Z}}(0|0) = \begin{bmatrix} \hat{\mathbf{X}}(0|0) \\ \hat{\dot{\mathbf{X}}}(0|0) \\ \tilde{\mathbf{K}}(0|0) \end{bmatrix} \quad (23)$$

The uncertainty in the assumption of the initial state mean is considered by an initial error covariance matrix $\mathbf{P}(0|0)$ defined as:

$$\mathbf{P}(0|0) = \begin{bmatrix} \mathbf{P}_s(0|0) & 0 \\ 0 & \mathbf{P}_p(0|0) \end{bmatrix} \quad (24)$$

The subscripts s and p are defined earlier. Generally, $\mathbf{P}_s(0|0)$ is considered to be a unit diagonal matrix as previously used by Hoshiya and Saito (1984), Koh et al. (1991), Wang and Haldar (1997). $\mathbf{P}_p(0|0)$ is a diagonal matrix with large numbers in the diagonals representing the uncertainty in their initial values; it will depend on the magnitude of the stiffness parameters of the structural members. Jazwinski (1970) commented that the large positive numbers for the covariance values for the system parameters accelerate the convergence of the local iteration. Thus, in this study $\mathbf{P}(0|0)$ is defined as:

$$\mathbf{P}(0|0)=\begin{bmatrix}\mathbf{I}_1 & 0\\ 0 & \lambda\mathbf{I}_2\end{bmatrix} \quad (25)$$

where $\mathbf{I}_1$ and $\mathbf{I}_2$ are unit matrices and λ is the large positive number assumed to be of the order of 1000.

The discussions clearly indicate that to start the filtering the information on $\hat{\mathbf{Z}}(0|0)$, $\mathbf{P}(0|0)$, and $\mathbf{R}$(k) is necessary.

After the uncertain initial conditions are assigned appropriately, the filtering process is performed in the following two steps:

(i) Prediction of new state mean and its new error covariance – The state mean $\hat{\mathbf{Z}}(k \mid k)$ and error covariance $\mathbf{P}(k \mid k)$ at time k are propagated one step forward in time to predict the new state mean $\hat{\mathbf{Z}}(k \mid k)$ and new error covariance $\mathbf{P}(k+1 \mid k)$ at time k+1 by numerically solving the fllowing differential equations as:

$$\hat{\mathbf{Z}}(k+1|k)=\hat{\mathbf{Z}}(k|k)+\int_{k\Delta t}^{(k+1)\Delta t} f(\mathbf{Z}(t|k),t)dt \quad (26)$$

$$\mathbf{P}(k+1|k)=\mathbf{\Phi}(k+1|k)\mathbf{P}(k|k)\mathbf{\Phi}^T(k+1|k)) \quad (27)$$

where $\mathbf{\Phi}(k+1|k)$ is the state transition matrix of the system. For small Δt, it can be approximately defined as:

$$\mathbf{\Phi}(k+1|k)=\mathbf{I}+\Delta t\left[\frac{\partial f((\mathbf{Z}(t),t)}{\partial \mathbf{Z}(t)}\right]_{\mathbf{Z}(t)=\hat{\mathbf{Z}}(k|k)} \quad (28)$$

All other terms were defined earlier. Numerical solution of Equation (26) will introduce the piece-wise linear approximation in the formulation.

(ii) Updating the predicted state mean and its error covariance – Using the available measurements at time k+1, the predicted state mean and error covariance are updated using the Kalman gain matrix $\mathbf{K}$(k+1) as:

$$\hat{\mathbf{Z}}(k+1|k+1)=\hat{\mathbf{Z}}(k+1|k)+ \cdot\mathbf{K}(k+1)[\mathbf{Y}(k+1)-\mathbf{H}\cdot\mathbf{Z}(k+1|k)] \quad (29)$$

$$\mathbf{P}(k+1|k+1)=[\mathbf{I}-\mathbf{K}(k+1)\mathbf{H}]\mathbf{P}(k+1|k)[\mathbf{I}-\mathbf{K}(k+1)\mathbf{H}]^T+ \mathbf{K}(k+1)\mathbf{R}(k+1)\mathbf{K}^T(k+1) \quad (30)$$

where

$$\mathbf{K}(k+1)=\mathbf{P}(k+1|k)\mathbf{H}^T[\mathbf{H}\mathbf{P}(k+1|k)\mathbf{H}^T+ \cdot\mathbf{R}(k+1)]^{-1} \quad (31)$$

As discussed earlier, for the purpose of structural identification, the dynamic responses will be measured at every Δt s time interval for a total duration of, say T s, providing a total of n samples. The prediction and updating operations described by Eq. 26 through Eq. 31 will be carried out locally for each of the time points, i.e., k = 1, 2, …, n, generally termed as the local iteration. When the local iteration is performed for all the time points in the entire time-history, it is denoted as global iteration procedure. Jazwinski (1970) suggested that the global iteration procedure should be repeated until the two successive states are essentially identical. After the completion of the first global iteration, considering the stability and convergence, Hoshiya and Saito (1984) proposed a weighted global iteration (WGI) scheme in the EKF procedure to be carried out in the subsequent global iterations. It is commonly known as the EKF-WGI procedure. It can be mathematically presented as:

$$\hat{\mathbf{Z}}^{(2)}(0|0)=\begin{bmatrix}\hat{\mathbf{X}}^{(2)}(0|0)\\ \hat{\mathbf{X}}^{(2)}(0|0)\\ \mathbf{K}^{(2)}(0|0)\end{bmatrix}=\begin{bmatrix}\hat{\mathbf{X}}^{(1)}(0|0)\\ \hat{\mathbf{X}}^{(1)}(0|0)\\ \mathbf{K}^{(1)}(n|n)\end{bmatrix} \quad (32)$$

$$\mathbf{P}^{(2)}(0|0)=\begin{bmatrix}\mathbf{I}_1 & 0\\ 0 & w\mathbf{P}^{(1)}(n|n)\end{bmatrix} \quad (33)$$

Steps in EKF-WGI procedure

The WGI method in the EKF-WGI procedure is carried out by scaling up the covariance values of the system parameters, obtained at the end of the previous global iteration, by a sufficiently large weight factor (w). This will satisfy the stability and convergence of the identified system

parameters towards the true solution. Following are the steps involved:

(i) Develop the initial state vector $\hat{\mathbf{Z}}(0|0)$ and error covariance matrix $\mathbf{P}(0|0)$ for the whole system as described in Eq. 23 and 24, respectively.

(ii) Carry out the local iterations comprising of the prediction and updating the state mean and error covariance in the EKF procedure for all the time steps considering k = 1, 2, …, n, completing the first global iteration producing the updated $\hat{\mathbf{Z}}^{(1)}(n|n)$ and $\mathbf{P}^{(1)}(n|n)$ at the end of the last time step.

(iii) As described in Eq. 32 and 33, define the initial state vector $\hat{\mathbf{Z}}^{(2)}(0|0)$ and error variance matrix $\mathbf{P}^{(2)}(0|0)$ for the second global iteration using the system parameters and their covariance values obtained in step (ii) by scaling up the covariance values by a large positive weight factor (w).

(iv) Carry out the local iteration steps of the EKF procedure within the second global iteration to obtain $\hat{\mathbf{Z}}^{(2)}(n|n)$ and $\mathbf{P}^{(2)}(n|n)$.

(iv) Continue the iterative procedure until the updated system parameters at the end of a global iteration show no longer improvement from their assumed values, ensuring the convergence of the parameters. In the numerical procedure in this study a value of 1% is used for estimated relative error (c) to stop the iteration process.

The covariance values provide a measure of the filter performance and indicate the stability of estimated states. The use of weight factor in the initial covariance matrix introduces high fluctuation of the state vector $\hat{\mathbf{Z}}(k|k)$ in the initial stage. Although the weight factor seemed to play an important role in the later stage to assure convergence (Hoshiya and Saito, 1984), the global iteration procedure does not essentially guarantee the convergence of the iteration scheme; in fact, it may diverge because of incorrect assumption of initial statē vector, modeling error, limitation of computer processing power, numerical precision, etc. (Jazwinski, 1970; Simon, 2006; Speyer and Chung, 2008). In any case, the stability and convergence of the estimated system parameters can be judged by the nature of an objective function (θ) (not presented here), as suggested by Hoshiya and Saito (1984). The same objective function is implemented in this study. When the identified system parameters tend to diverge, the best estimated values are obtained corresponding to the minimum objective function.

4. Examples

4.1 Health assessment of a 3D frame

Health assessment processes of a 3D frame considering defect-free and various defective states are presented in the following sections.

Description of the Frame

A 3D three-story frame with square base of sides 9.14 m each and story height of 3.66 m, as shown in Fig. 1, is considered. The beams and columns are made of W21x68 and W14x61sections, respectively, of Grade 50 steel. In FE representation, the frame is represented by 16 nodes, denoted by numbers in regular typescript, and 24 elements, denoted by numbers in italic typescript with underline. For easier visualization, the elements in the two back sides are shown by dotted lines. All the elements are considered to be three dimensional beam elements with rigid connections. The support condition at the base of the frame (node 13, 14, 15, 16) is considered to be fixed. Each node has six DDOFs: three translational and three rotational. Thus, the total number of DDOFs for the frame is 72. The actual theoretical stiffness parameters k_i defined in terms of (E_iI_{zi}/L_i) are calculated to be 13476 kN-m and 14553 kN-m for a typical beam and a column, respectively. First two natural frequencies of the frame are estimated to be f_1 = 2.7229 Hz and f_2 = 3.5717 Hz, respectively. Following the procedure described in Clough and Penzien (1993), Rayleigh damping coefficient α and β are calculated to be 0.97077 and 0.0025284, respectively, for an equivalent modal damping of 5% (commonly used in model codes in the U.S.) of the critical for the first two modes.

Supposed structural responses are measured at all DDOFs in the substructure. The task is to identify stiffness parameters of all 24 elements using responses measured only in the substructure, i.e., at nodes 1, 2, 3, and 5.

During an actual inspection, the responses will be measured. For this illustrative example to demonstrate the application potential of the 3D GILS-EKF-UI procedure, responses are generated numerically for theoretical verification. The frame is excited by a sinusoidal load $f(t) = 10\sin(20t)$ kN, applied at node 1 in the horizontal direction as shown in Fig. 1. Responses are analytically generated using a commercial software ANSYS (ver. 11). After the responses are generated, the information on the excitation force is completely ignored. The responses are generated at every 0.0001 s time interval. Responses between 0.31 s and 0.63 s, providing 3201 samples are used in this example to assess the health of the 3D frame.

4.2 Health assessment of defect-free frame

Using only responses at four nodes in the substructure, the stiffness and damping parameters and the time-history of unknown input force are identified using the 3D GILS-UI procedure in Stage 1. The identified stiffness parameters and the errors in identification are shown in columns 3 and 4 of Table 1(a), respectively. As commonly used in the literature, the errors are defined as the percentage deviation of identified values (at the current state) with respect to the initial theoretical values used to generate the response information. In actual field inspections, the information can be obtained from design drawings, or from previous inspections, if available. The errors in the stiffness parameter identification of the three members in the substructure are very small. The excitation time history was also identified very accurately, but not shown here for the sake of brevity.

The stiffness parameters of all 24 elements of the frame are then estimated using the 3D GILS-EKF-UI procedure in Stage 2 using only responses at nodes 1, 2, 3, and 5. The identified stiffness parameters and corresponding errors are shown in columns 3 and 4 of Table 1(b). The magnitudes of errors are large and varied significantly from members to members; obviously, the method failed to identify the defect-free state of the frame. To identify all the stiffness parameters, the EKF algorithm calculates the responses at all the DDOFs in the whole structure using the piece-wise linear approximation in the mathematical formulation and then update the information using the measured responses. Obviously, the accuracy in the identification increases with the increase in the number of measured responses. Observing the errors in the identified stiffness parameters, it can be concluded that the measured responses at 24 DDOFs are not sufficient enough to generate responses at the rest of the DDOFs. To improve the accuracy, it is essential to obtain additional observations besides at the substructure. This is the basic challenge in the EKF procedure since during an actual field inspections, it will be extremely difficult to decide the absolute minimum number of required responses for the successful identification. Furthermore, it is expected to be different for different structures and will greatly depend on the experience of the inspectors. It will cost more money to measure additional responses. In this numerical study, a scaling approach suggested by Vo and Haldar (2004), is used to explore the possibility of avoiding measuring additional responses. An extensive numerical study on different types of structures indicates that if the responses are assumed to be linear, as expected during the inspection, structural responses at one node can be scaled from other nodes. This is also found to be valid for the frame under consideration. It is observed that responses at nodes 4 and 6 are almost identical to responses at nodes 3 and 5, respectively; indicating that the responses at nodes 4 and 6 can be scaled from the responses measured at nodes 3 and 5 to facilitate the identification process in stage 2. Two additional responses (out-of plane translation and rotation about the horizontal axis in the plane of the paper (see Fig. 1) at nodes 7 and 8 can be scaled using the responses at node 5. Following this concept, additional responses at 16 DDOFs can also be generated without conducting any experiments. Thus, the total number of measured responses can be increased from 24 to 40 without spending any additional resources. Using 40 responses and 3D GILS-EKF-UI, the identified stiffness parameters and corresponding errors in the identification are shown columns

Table 1. Stiffness parameter (k_i) identification of defect-free frame using 3D GILS-EKF-UI

(a) Stage 1 – Identification of the substructure

Element (k_i)	Theoretical values	Identified values	Error (%)
(1)	(2)	(3)	(4)
1-2 (k_1)	13476	13476	-0.003
1-3 (k_7)	13476	13476	-0.001
1-5 (k_{13})	14553	14553	-0.001

(b) Stage 2 – Identification of the whole frame

Element (k_i)	Theoretical values	24 DDOFs		40 DDOFs	
		Identified values	Error (%)	Identified values	Error (%)
(1)	(2)	(3)	(4)	(5)	(6)
1-2 (k_1)	13476	13580	0.77	13485	0.06
5-6 (k_2)	13476	12316	-8.61	13482	0.04
9-10 (k_3)	13476	23452	74.02	13599	0.91
3-4 (k_4)	13476	9658	-28.33	13520	0.33
7-8 (k_5)	13476	21654	60.68	13305	-1.27
11-12 (k_6)	13476	14635	8.60	13859	2.84
1-3 (k_7)	13476	13711	1.74	13480	0.03
5-7 (k_8)	13476	11807	-12.39	13478	0.01
9-11 (k_9)	13476	16447	22.05	13578	0.76
2-4 (k_{10})	13476	11339	-15.86	13499	0.17
6-8 (k_{11})	13476	24227	79.78	13459	-0.13
10-12 (k_{12})	13476	13928	3.35	13549	0.54
1-5 (k_{13})	14553	14953	2.75	14548	-0.03
3-7 (k_{14})	14553	10757	-26.08	14655	0.70
5-9 (k_{15})	14553	11931	-18.02	14572	0.13
7-11 (k_{16})	14553	26546	82.41	14513	-0.28
9-13 (k_{17})	14553	14476	-0.53	14500	-0.36
11-15 (k_{18})	14553	17089	17.43	14438	-0.79
2-6 (k_{19})	14553	15075	3.58	14567	0.10
4-8 (k_{20})	14553	11938	-17.97	14625	0.49
6-10 (k_{21})	14553	14338	-1.48	14567	0.09
8-12 (k_{22})	14553	14852	2.06	14423	-0.89
10-14 (k_{23})	14553	13171	-9.49	14532	-0.14
12-16 (k_{24})	14553	7827	-46.22	14573	0.14

5 and 6 in Table 1b. The maximum error in the identification is reduced from 82.41% to 2.84%, indicating the benefit of additional responses. In fact, if responses are available at all 72 DDOFs, the maximum error in the identification is expected to be similar to that observed for the substructure. In the subsequent discussions, identified stiffness parameter values will be given considering responses available at 40 DDOFs. In this example, since the error values are very small and do not change significantly from members to members, it is implied that the frame is defect-free and 3D GILS-EKF-UI correctly identified the defect-free state of the frame.

Table 2. Stiffness parameter (k_i) identification defective frames using 3D GILS-EKF-UI

(a) Stage 1 – Identification of the substructures

Element (k_i)	Theoretical values	20% thickness reduction for 5-6		50% thickness reduction for 5-6		99% thickness reduction for 5-6	
		Identified values	Error (%)	Identified values	Error (%)	Identified values	Error (%)
(1)	(2)	(3)	(4)	(5)	(6)	(7)	(8)
1-2 (k_1)	13476	13476	-0.003	13476	-0.003	13476	-0.003
1-3 (k_7)	13476	13476	-0.001	13476	-0.001	13476	-0.002
1-5 (k_{13})	14553	14553	-0.001	14553	-0.001	14553	-0.002

(b) Stage 2 – Identification of the whole frames

Element (k_i)	Theoretical values	20% thickness reduction for 5-6		50% thickness reduction for 5-6		99% thickness reduction for 5-6	
		Identified alues	Error (%)	Identified values	Error (%)	Identified values	Error (%)
(1)	(2)	(3)	(4)	(5)	(6)	(7)	(8)
1-2 (k_1)	13476	13516	0.30	13522	0.34	13514	0.28
5-6 (k_2)	13476	10471	**-22.30**	6436	**-52.24**	128	**-99.05**
9-10 (k_3)	13476	15086	11.94	14967	11.06	13530	0.40
3-4 (k_4)	13476	13604	0.95	13578	0.75	13570	0.69
7-8 (k_5)	13476	13120	-2.64	13216	-1.93	13141	-2.49
11-12 (k_6)	13476	14219	5.51	14157	5.05	15437	14.55
1-3 (k_7)	13476	13492	0.12	13495	0.14	13521	0.33
5-7 (k_8)	13476	13384	-0.69	13363	-0.84	13400	-0.57
9-11 (k_9)	13476	13809	2.47	13839	2.69	14008	3.95
2-4 (k_{10})	13476	13509	0.25	13513	0.27	13513	0.27
6-8 (k_{11})	13476	13362	-0.85	13337	-1.03	13442	-0.25
10-12 (k_{12})	13476	13752	2.05	13777	2.23	13909	3.21
1-5 (k_{13})	14553	14545	-0.05	14545	-0.05	14515	-0.26
3-7 (k_{14})	14553	14562	0.06	14537	-0.11	14741	1.29
5-9 (k_{15})	14553	14589	0.25	14609	0.39	14660	0.74
7-11 (k_{16})	14553	14516	-0.25	14562	0.06	14305	-1.71
9-13 (k_{17})	14553	14161	-2.69	14167	-2.65	14457	-0.66
11-15 (k_{18})	14553	14352	-1.38	14320	-1.60	14191	-2.49
2-6 (k_{19})	14553	14563	0.07	14564	0.08	14571	0.13
4-8 (k_{20})	14553	14509	-0.30	14481	-0.49	14738	1.27
6-10 (k_{21})	14553	14582	0.20	14597	0.30	14697	0.99
8-12 (k_{22})	14553	14302	-1.72	14322	-1.59	14135	-2.87
10-14 (k_{23})	14553	14197	-2.45	14206	-2.39	14433	-0.82
12-16 (k_{24})	14553	14640	0.60	14649	0.66	14423	-0.89

4.3 Health assessment of defective frames

After successful identification of the defect-free frame, a member 2, between node 5 and 6, is assumed to be corroded or defective. Experience gained from laboratory experiments (Marinez-Flores and Haldar, 2007; Martinez-Flores et al., 2008), prompted the authors to consider three (low, moderate, and severe) defective states by reducing the thicknesses of web and flange of member 2 by 20%, 50%, and 99%, respectively. Similar cases were used by Marinez-Flores and Haldar (2007) and Martinez-Flores et al., (2008) for 2D frames, in their experimental investigations.

The reduction in the web and flange thicknesses caused the reduction in the principal moment of inertias about major axis (I_z) by 22.15%, 52.14%, and 99.07%, respectively; principal moment of inertias about the minor axis (I_y) by 20.05%, 50.07%, and 99.0%, respectively; and cross-sectional areas (A) by 20.74%, 50.47%, and 99.01%, respectively. The FE model of the frame and the substructure for the three cases remain same as in the defect-free case. Using the reduced cross sectional properties of member 2 and using ANSYS, the analytical responses were generated as before for the three defective states. Using responses measured between 0.31 s and 0.63 s at node 1, 2, 3, and 5, the substructures for the three defective cases are identified and the results are summarized in columns 3, 5, and 7 of Table 2(a). Obviously, the substructures are identified very accurately. As discussed before, using 40 responses between 0.31 s and 0.63 s, all 24 elements in the frame are identified for the three defective states and the results are shown in column 3, 5, and 7 of Table 2(b). The identified stiffness parameter for member 2 reduces by 22.30%, 52.24%, and 99.05%, respectively, for the three defective cases. The reductions are much higher than other 23 members, indicating location and severity of the defect. It can be concluded that 3D-GILS-EKF-UI also correctly identified the three defective states.

It is to be noted that for this example, the defective member is not in the substructure. Our experience indicates that if it were in the substructure, the defect identification capability of 3D-GILS-EKF-UI will improve significantly. On the other hand, if the defective member is further away from the substructure, the defect identification capability of the method will reduce. In this example, the defective member is close to the substructure and the defect identification capability of 3D-GILS-EKF-UI did not suffer. The example also demonstrated that the defective member need not be in the substructure. The method can be used to identify multiple defective members. Since locations of defects may not be known prior to inspection, in most cases, the authors recommend using multiple substructures, assuring that defect locations will be close to at least one of them.

5. Conclusions

A finite-elements-based time domain system identification technique, denoted as 3D GILS-EKF-UI, is developed in this paper for health assessment of three dimensional structures. The method uses dynamic response information and integrates an iterative least-squares technique and the extended Kalman filter-based concept for detecting location(s) of defect(s) and their severity for the rapid assessment of structural health. It tracks the changes in stiffness parameters at the finite element level. The unique features of the procedure are that it does not require information on dynamic excitation and uses noise-contaminated responses measured only at small part(s) of the structure. The required mathematics are developed using a two-stage approach. With the help of examples, it is demonstrated that the method is capable of accurately identifying defect-free and defective states of three dimensional structures. The method addresses several implementation issues for rapid, economical, and easier assessment of structural health. Considering the accuracy and robustness, it is expected that the procedure can be used as a vibration-based nondestructive health assessment procedure.

References

1. ANSYS version 11.0, The Engineering Solutions Company, 2007.
2. Carden, E. P., and Fanning, P. (2004), "Vibration based condition monitoring: a review," Structural Health Monitoring, 3(4), 355-377.

3. Clough, R. W., and Penzien, J. (1993), "Dynamics of structures," Second Edition, McGraw-Hill, New York, USA.
4. Das, A. K., Haldar, A., and Chakraborty, S. (2012), "Health assessment of large two dimensional structures using minimum information – recent advances," Advances in Civil Engineering, Volume 2012, Article ID 582472, doi:10.1155/2012/582472.
5. Doebling, S. W., Farrar, C. R., Prime, M. B., and Shevitz, D. W. (1996), "Damage identification and health monitoring of structural and mechanical systems from changes in their vibration characteristics: a literature review," Los Alamos National Laboratory, Report No. LA-13070-MS.
6. Fan, W., and Qiao, P. (2010), "Vibration-based damage identification methods: a review and comparative study," Structural Health Monitoring, 0(0), 1-29.
7. Farrar, C. R., and Doebling, S. W. (1997), "A review of modal-based damage identification procedures," Los Alamos National Laboratory, LA-UR-97-2468.
8. Fritzen, C-P (2006), "Vibration-based techniques for structural health monitoring," Chapter 2, Structural Health Monitoring, Edited by: Daniel Balageas, Claus-Peter Fritzen, Alfredo Güemes, ISTE Ltd, USA.
9. Ghanem, R., and Shinozuka, M. (1995), "Structural-system identification. I: theory," Journal of Engineering Mechanics, 121(2), 255-264.
10. Hoshiya, M., and Saito, E. (1984), "Structural identification by extended Kalman filter," Journal of Engineering Mechanics, ASCE, 110(12), 1757-1770.
11. Humar, J., Bagchi, A., and Xu, H. (2006), "Performance of vibration-based techniques for the identification of structural damage," Structural Health Monitoring, 5(3), 215-241.
12. Jazwinski, A. H. (1970), "Stochastic process and filtering theory," Academic Press, Inc., United Kingdom.
13. Katkhuda, H., and Haldar, A. (2008), "A novel health assessment technique with minimum information," Structural Control & Health Monitoring, 15(6), 821-838.
14. Katkhuda, H., Martinez-Flores, R., and Haldar, A. (2005), "Health assessment at local level with unknown input excitation," Journal of Struct. Engineering, 131(6), 956-965.
15. Kerschen, G., Worden, K., Vakakis, A. F., and Golinval, J. C. (2006), "Past, present and future of nonlinear system identification in structural dynamics," Mechanical Systems and Signal Processing, 20(3), 505-592.
16. Koh, C. G., See, L. M., and Balendra, T. (1991), "Estimation of structural parameters in time domain: a substructural approach," Earthquake Engineering and Structural Dynamics, 20, 787-801.
17. Lew, J. S., Juang, J. N., and Longman, R. W. (1993), "Comparison of several system identification methods for flexible structures," Journal of Sound and Vibration, 167(3), 461-480.
18. Ling, X., and Haldar, A. (2004), "Element level system identification with unknown input with Rayleigh damping," Journal of Engrg Mech., ASCE, 130(8), 877-885.
19. Martinez-Flores, R., and Haldar, A. (2007), "Experimental verification of a structural health assessment method without excitation information," Journal of Structural Engineering, 34(1), 33-39.
20. Martinez-Flores, R., Katkhuda, H., and Haldar, A. (2008), "A novel health assessment technique with minimum information: verification," International Journal of Performability Engineering, 4(2), 121-140.
21. Nasrellah, H. A. (2009), "Dynamic state estimation techniques for identification of parameters of finite element structural models," Doctoral Dissertation, Indian Institute of Science, Bangalore, India.
22. Paz, M. (1985), "Structural dynamics: theory and computation," second edition, Van Nostrand Reinhold Company, New York, USA.
23. Salawu, O. S. (1997), "Detection of structural damage through changes in frequency: a review," Engineering Structures, 19(9), 718-723.
24. Saridis, G. N. (1995), "Stochastic processes, estimation, and control: the entropy approach," John Wiley & Sons, Inc., New York, USA.
25. Shinozuka, M., and Ghanem, R. (1995), "Structural system identification. II: experimental verification," Journal of Engineering Mechanics, 121(2), 265-273.
26. Simon, D. (2006), "Optimal state estimation: Kalman, H_μ and nonlinear approaches," John Wiley and Sons, Inc., Hoboken, New Jersey, USA.
27. Sohn, H., Farrar, C. R., Hemez, F. M., Shunk, D. D., Stinemates, D. W., Nadler, B. R., and Czarnecki, J. J. (2004), "A review of structural health monitoring literature: 1996-2001," Los Alamos National Laboratory, LA-13976-MS.
28. Speyer, J. L., and Chung, W. H. (2008), "Stochastic processes, estimation, and control," Society for Industrial and Applied Mathematics, Philadelphia, USA.
29. Vo, P. H., and Haldar, A. (2003), "Post processing of linear accelerometer data in system identification," Journal of Structural Engineering, 30(2), 123-130.
30. Vo, P. H., and Haldar, A. (2004), "Health assessment of beams - theoretical and experimental investigation," Journal of Structural Engineering, Special issue on Advances in Health Monitoring/Assessment of Structures including Heritage and Monument Structures, 31(1), 23-30.
31. Wang, D., and Haldar, A. (1994), "An element level SI with unknown input information," Journal of Engineering Mechanics, ASCE, 120(1), 159-176.
32. Wang, D., and Haldar, A. (1997), "System identification with limited observations and without input," Journal of Engineering Mechanics, 123(5), 504-511.

Life Cycle Reliability and Safety Engineering
Vol.1 Issue 1 (2012) 15-25

Atoms and Molecules in Mirce Mechanics Approach to Reliability

J. Knezevic
MIRCE Akademy, Exeter, EX5 1JJ, UK.

Abstract

Although reliability is defined through probability characteristics, the full understanding of it is only possible by observing, analysing and understanding failures of systems, which are defined as negative functionability events in Mirce Mechanics. Thus, this paper presents the fundamental properties of atoms and molecules, as a prerequisite for the scientific understanding of functionability phenomena that lead to the occurrence of negative functionability events during the life of a system.

Keyword : *Reliability physics, Science of reliability, Physics-of- failure*

1. Introduction

It is commonly accepted that reliability is defined as a probability that a system will maintain a required function during a stated period of time. As a probability cannot be seen or measured directly there seems to be a certain fundamental difficulty in understanding and interpreting statistical and probability functions in real life. This is because physical characteristics of a system like the weight, temperature, volume and similar have a clear and measurable meaning. However, the concepts of probability, and hence reliability, is an abstract property of a system that obtains a physical meaning only when behaviour of a large sample of systems is considered. Hence, understanding of reliability is reduced to the physical observation and analysis of system failures, which are observable and measurable physical characteristics.

According to the Mirce Mechanics, system failures are negative functionability events that cause transition of a system from positive to negative functionability state [1] due to some of the following reasons, or combinations of them:

a) Built-in design errors (incorrect selection of materials, stresses shapes, etc)
b) Production errors (human errors in assembly, delivery and installation tasks)
c) Irreversible changes in the condition of components with time due to wear, fatigue, creep, corrosion, and similar degradation processes
d) Imposition of external stresses resulting from collisions, harsh landings, extreme weather conditions, etc
e) Human errors in execution of maintenance tasks
f) Human errors in execution of in-service support tasks

At the MIRCE Akademy a large number of negative functionability events and associated phenomena have been observed and analysed to understand the physical mechanisms that leads to their occurrences.

Consequently, systematic studies are applied to understand phenomena that cause thermal aging, thermal buckling, photo-chemical degradation, reduction in dielectric strength, evaporation, metal fatigue, actinic degradation, photo-oxidation, swelling/ shrinking, degradation of optical qualities, fogging, photochemical decomposition of paint, blistering, warping, thermal stress, breakdown of lubrication film, increased structural loads, shift in the centre of gravity, jammed control surfaces, attenuation of energy, clutter echoes, blocking of air intakes, decreased lift and increased drag, unequal loading, removal of coating protection, pitting, roughening of the surface, acid reactions, leakage currents, promotion of mould growth, reduction

of heat transfer, caking and drying, premature cracking, hot spots creation, erosion, bleaching preservatives, abrasive wear, corrosion, alkaline reactions and similar.

For years, research studies, international conferences, summer schools and other events have been organised in order to understand just a physical scale at which failure phenomena should be studied and understood. In order to understand the motion of negative functionability events it is necessary to understand the physical mechanisms of that motion. That represented a real challenge, as the answers to the question "what are physical and chemical processes that lead to the occurrence of negative functionability events" have to be provided. Without accurate answers to those questions the prediction of their future occurrences is not possible, and without ability to predict the future, the use of the word science becomes inappropriate.

After a numerous discussions, studies and trials, it has been concluded that any serious studies in this direction, from Mirce Mechanics point of view, have to be based between the following two boundaries:

- the "bottom end" of the physical world, which is at the level of the atoms and molecules that exists in the region of 10^{-10} of a metre [3],
- the "top end" of the physical world, which is at the level of the solar system that stretches in the physical scale around 10^{+10} of a metre. [4]

This range is the minimum sufficient "physical scale" which enables scientific understanding of relationships between system functionability processes and system functionability events.

As matter is composed of atoms, its property is a consequence of the manner in which the atomic elements are arranged into molecules. Consequently, the main objective of this paper is to argue that the scientific approach to reliability is the only way forward for all members of the reliability community who wish to make accurate predictions that will be confirmed during the operational processes of the future systems. For that to happen scientific understanding of failure phenomena is required. This paper advocates that research of this nature must start with the understanding of the properties of atoms and their bonding to form molecules, in order for negative functionability events to be understood. Then and only then, accurate and meaningful reliability predictions become possible, which finally leads to the reduction of the probability of the occurrence of negative functionability events during the life of a system.

2. Electronic Structure of an Atom

The understanding and prediction of the properties of matter at the atomic level represents one of the great achievements of twentieth-century science. As matter is composed of atoms, this paper starts with its property and the manner in which the atomic elements are arranged. Electron density describes the distribution of the electronic charge throughout real space resulting from the attractive forces generated by nuclei. It is a measurable property that determines the appearance and form of matter. The theory developed to describe the behaviour of electrons, atoms and molecules differs radically from known Newtonian physics, which governs the motions of macroscopic bodies and the physical events of our everyday experiences. That new theory, which is able to account for all observable behaviour of matter, was named quantum mechanics.

The proper formulation of quantum mechanics and its application to a specific problem requires a rather elaborate mathematical framework, as do proper statements and applications of Newtonian physics. Hence, principles of quantum mechanics and its basic concepts are used for the studies of the motion and relationship between atoms in molecules. Thus, the physical laws governing the behaviour of electrons and their arrangements, when bound to nuclei, to form atoms and molecules have been discovered, and termed the electronic structure of the atom or molecule. Furthermore, understanding of the relationship between the electronic structure of an atom and its physical properties enables understanding of the change

of electronic structure during a chemical reaction, where only the number and arrangement of the electrons are changed while the nucleus remaining unaltered. Thus, the unchanging charge of the atomic nucleus is responsible for retaining the atom's chemical identity through any chemical reaction. Therefore, for the purpose of understanding the chemical properties and behaviour of atoms, the nucleus may be regarded as simply a point charge of constant magnitude for a given element, giving rise to a central field of force that binds the electrons to the atom. [2]

3. Atomic Phenomena

Rutherford's nuclear model for the atom set the stage for the understanding of the structure of atoms and the forces holding them together. From Rutherford's alpha-scattering experiments it was clear that the atom consisted of a positively-charged nucleus with negatively-charged electrons arranged in some fashion around it, the electrons occupying a volume of space many times larger than that occupied by the nucleus. The diameters of nuclei fall in the range of 1×10^{-14} to 1×10^{-15} m, while the diameter of an atom is typically of the order of magnitude of 1×10^{-10} m. The forces responsible for binding the atom, and in fact all matter apart from the nuclei themselves, are electrostatic in origin: the positively charged nucleus attracts the negatively charged electrons. There are attendant magnetic forces that arise from the motions of the charged particles. These magnetic forces give rise to many important physical phenomena, but they are smaller in magnitude than are the electrostatic forces and they are not responsible for the binding found in matter.

4. Single Atom Structure

When a stable atom is formed, the electron is attracted to the nucleus, and as the radius is less than infinity, the energy has a negative sign, which implies that it must be supplied to the system if the electron is to overcome the attractive force of the nucleus and escape from the atom.

The motion of the electron is not free. The electron is bound to the atom by the attractive force of the nucleus and consequently quantum mechanics predicts that the total energy of the electron is quantised and equal to $E_n = \left(-2\pi^2 me^4 Z^2\right)/\left(n^2h^2\right)$, $n = 1, 2, 3, \ldots..$, where m is the mass of the electron, e is the magnitude of the electronic charge, n is a quantum number, h is Planck's constant and Z is the atomic number, which is the number of positive charges in the nucleus.

Since the motion of the electron occurs in three dimensions it is correct to anticipate three quantum numbers for the hydrogen atom. However, as the energy depends only on the quantum number n it is called the principal quantum number. When n is equal to infinity and energy is equal to zero the electron is free of the attractive force of the nucleus. The average distance between the nucleus and the electron increases as the energy or the value of n increases. Hence, energy must be supplied to pull the electron away from the nucleus.

4.1 The Probability Distributions for the Hydrogen Atom

To what extent is possible to pinpoint the position of an electron when it is bound to an atom? An order of magnitude for the answer to this question could be obtained by applying the uncertainty principle $\Delta x \Delta p = h$ to estimate Δx. The value of Δx represents the minimum uncertainty in our knowledge of the position of the electron. The momentum of an electron in an atom is of the order of magnitude of $9\text{x}10^{-19}$ g cm/sec. The uncertainty in the momentum Δp must necessarily be of the same order of magnitude. According to Bader [2] the answer is $\Delta x = 7\times10^{-27}/9\times10^{-19} \approx 10^{-8}$ cm.

The uncertainty in the position of the electron is of the same order of magnitude as the diameter of the atom itself. As long as the electron is bound to the atom, it is not possible to say much more about its position than that it is in the atom. This fact invalidated all models of the atom that describe the electron, as a particle following a definite trajectory or orbit.

Energy and one or more wave functions could be obtained for every value of *n*, the principal quantum number, by solving Schrödinger's

equation for the hydrogen atom. Knowledge of the wave functions, or probability amplitudes, allows calculation of the probability distributions for the electron in any given quantum level. When n=1, the wave function and the derived probability function are independent of direction and depend only on the distance between the electron and the nucleus.

An experiment designed to detect the position of the electron with an uncertainty much less than the diameter of the atom itself, when repeated a large number of times, shown that the electron is detected close to the nucleus most frequently and the probability of observing it at some distance from the nucleus decreases rapidly with increasing radial distance [2]. The atom was ionised in making each of these observations because the energy of the photons with a wavelength much less than 10^{-8} cm is greater than the amount of energy required to ionise the hydrogen atom. If light with a wavelength comparable to the diameter of the atom was used in the experiment, then the electron would not have been excited and the knowledge of its position would have been correspondingly less precise.

When the electron is in a definite energy level, the electron density distributions describe the manner in which the total electronic charge is distributed in space. The electron density is expressed in terms of the number of electronic charges per unit volume of space, e-/V. The volume V is usually expressed in atomic units of length cubed, and one atomic unit of electron density is then e^-/a_0^3. To give an idea of the order of magnitude of an atomic density unit, 1 au of charge density $e^-/a_0^3 = 6.7$ electronic charges per 10^{-8} cm^3. That is, a cube with a length of 0.52917×10^{-8} cm, if uniformly filled with an electronic charge density of 1 au, would contain 6.7 electronic charges.

The important point of the above discussion is that both the angular momentum and the energy of an atom remain constant if the atom is left undisturbed. Any physical quantity that is constant in a classical system is both conserved and quantised in a quantum mechanical system. Thus both the energy and the angular momentum are quantised for an atom.

Since an electron may exhibit a magnetic moment even when it does not possess orbital angular momentum, it must possess some internal motion. This motion is known as the electron spin and it is treated in quantum mechanics as another kind of angular momentum. Experimentally, however, all that is known is that the electron possesses an intrinsic magnetic moment. The remarkable feature of this intrinsic magnetic moment is that its magnitude and the number of components along a given axis are fixed. A given electron may exhibit only one of two possible components; it may be aligned with the field or against it. Hence only one quantum number is required to describe completely the spin properties of a single electron.

Finally, a total of four quantum numbers is required to specify completely the state of an electron when it is bound to an atom. The quantum numbers n, l and m determine its energy, orbital angular momentum and its component of orbital angular momentum. The fourth quantum number, the spin quantum number, summarises all that can be known about the spin angular momentum of the electron.

5. Pauli Exclusion Principle

The study of the magnetic properties of the ground and excited states of helium is sufficient to point out a general principle. For the ground state of helium, in which both electrons are in the same atomic orbital, only the non-magnetic form exists. This would imply that when two electrons are in the same atomic orbital their spins must be paired, that is, one up and one down. This is an experimental fact because helium is never found to be magnetic when it is in its electronic ground state. When the electrons are in different orbitals, then it is again an experimental fact that their spins may now be either paired or unpaired. This lead to the creation of the Pauli Exclusion Principle that states: no two electrons in the same atom may have all four quantum numbers the same. The Pauli principle cannot be derived from, nor is it predicted by, quantum

mechanics. It is a law of nature that must be taken into account along with quantum mechanics if the properties of matter are to be correctly described. The concept of atomic orbitals, as derived from quantum mechanics, together with the Pauli Exclusion Principle that limits the occupation of a given orbital, provides an understanding of the electronic structure of many-electron atoms. [2]

The concept of atomic orbitals in conjunction with the Pauli principle has indeed predicted a periodicity in the electronic structures of the elements. The form of this periodicity replicates exactly that one found in the Mendeleev's periodic table of the elements in which the periodicity is founded on the observed chemical and physical properties of the elements.

The diameter of an atom is difficult to define precisely as the density distribution tails off at large distances. However, there is a limit as to how close two atoms can be pushed together in a solid material. The size of the atom in general decreases as the number of electrons in the quantum shell increases. This observation, which at first sight might appear surprising, finds a ready explanation through the concept of an effective nuclear charge.

The electric field and hence the attractive force exerted by the nucleus on an electron in the outer quantum shell is reduced because of the screening effect of the other electrons which are present in the atom. An outer electron does not penetrate to any great extent the tightly bound density distribution of the inner shell electrons. Hence, each inner electron, which is an electron with an n value less than the n value of the electron in question, reduces the value of the nuclear charge experienced by the outer electron by almost one unit. The remaining outer electrons on the other hand are, on the average, all at the same distance away from the nucleus as is the electron under consideration. Consequently each outer electron screens considerably less than one nuclear charge from the other outer electrons. Thus the higher the ratio of outer shell to inner shell electrons, the larger is the "effective nuclear charge" which is experienced by an electron in the outer shell. [2]

6. Chemical Implications of Effective Nuclear Charge

The effective nuclear charge is a minimum for the group I elements in any given row of the periodic table. Therefore, it requires less energy to remove an outer electron from one of these elements than from any other element in the periodic table. The strong reducing ability of these elements is readily accounted for. The variation in the relative reducing power of the elements across a given period or within a given group is determined by the variation in the effective nuclear charge. The ability of the elements in a given row of the periodic table to act as reducing agents should undergo a continuous decrease from group I to group VII, since the effective nuclear charge increases across a given row. Similarly, the reducing ability should increase down a given column (group) in the table since the effective nuclear charge decreases as the principal quantum number is increased. Anticipating the fact that electrons can be transferred from one atom (the reducing agent) to another (the oxidizing agent) during a chemical reaction, it is expected that the elements to the left of the periodic table to exhibit a strong tendency to form positively charged ions.

The ability of the elements to act as oxidising agents should parallel directly the variations in the effective nuclear charge. Thus the oxidising ability should increase across a given row (from group I to group VII) and decreases down a given family. These trends are, of course, just the opposite of those noted for the reducing ability. The reducing ability should vary inversely with the ionisation potential, and the oxidising ability should vary directly with the electron affinity. The elements in groups VI and VII should exhibit a strong tendency for accepting electrons in chemical reactions to form negatively charged ions. For example, Francium, which possesses a single outer electron in the 7*s* orbital, is the strongest chemical reducing agent and fluorine, with an orbital vacancy in the 2*p* subshell is the strongest oxidizing agent. These are only a few examples of how knowledge of the electronic structure of atoms may be used to understand and correlate a large amount of chemical information

that certainly has significant impact of the failure mechanisms affecting the reliability of systems and their components. [2]

It should be pointed out that chemistry is a study of very complex interactions and the few simple concepts advanced here cannot begin to account for the incredible variety of phenomena actually observed.

7. The Chemical Bond

With understanding of the electronic structure of atoms, only briefly summarised above, it is possible to understand the existence of molecules. Clearly, the force that binds the atoms together to form a molecule is, as in the atomic case, the electrostatic force of attraction between the nuclei and electrons. In a molecule, however, a force of repulsion between the nuclei in addition to that between the electrons is encounter. To account for the existence of molecules it is necessary to account for the predominance of the attractive interactions, which could be shown in terms of the energy of a molecule, relative to the energies of the constituent atoms, and in terms of the forces acting on the nuclei in a molecule.

In order to determine what attractive and repulsive interactions are possible in a molecule, an instantaneous configuration of the nuclei and electrons in a hydrogen molecule is considered, as shown in Figure 1.When the two atoms are initially far apart, the distance *R* is very large, the only potential interactions are the attraction of nucleus A for electron number (1) and the attraction of nucleus B for electron number (2). When *R* is comparable to the diameter of an atom (A and B are close enough to form a molecule) then new interactions appear. Nucleus A now attracts electron (2) as well as (1) and similarly nucleus B attracts electron (1) as well as (2). The dashed lines represent the repulsive interactions between like charges and the solid lines indicate the attractive interactions between opposite charges.

The number of attractive interactions has been doubled from what it was when the atoms were far apart. However, the reduction in *R* introduces two repulsive interactions as well,

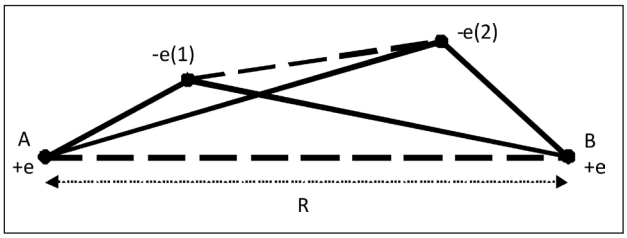

Figure 1: *One possible set of the instantaneous relative positions of the electrons and nuclei in a hydrogen molecule. [2]*

namely the two electrons now repel one another as do the two nuclei. If the two atoms are to remain together to form a molecule, the attractive interactions must exceed the repulsive ones. It is clear from Figure 1 that the new attractive interactions, nucleus A attracting electron (2) and nucleus B attracting electron (1), is large only if there is a high probability of both electrons being found in the region between the nuclei. When the average potential energy is calculated by quantum mechanics, the attractive interactions are found to predominate over the repulsive ones because quantum mechanics does indeed predict a high probability for each electron being in the region between the nuclei. This general consideration of the energy demonstrates that electron density must be concentrated between the nuclei if a stable molecule is to be formed, for only in this way can the attractive interaction be maximised.

In the atomic case it is possible to fix the position of the nucleus in space and consider only the motion of the electrons relative to the nucleus. However, in molecules, the nuclei may also change positions relative to one another. This additional movement can be neglected as the nuclei are very massive compared to the electrons and their average velocities are consequently much smaller than those possessed by the electrons. In a classical picture of the molecule we would see a slow, lumbering motion of the nuclei accompanied by a very rapid motion of the electrons. The physical implication of this large disparity in the two sets of velocities is that the electrons can immediately adjust to any change in the position of the nuclei. The positions of the nuclei determine the potential field in which the electrons move. However, as the nuclei change

their positions and hence the potential field, the electrons can immediately adjust to the new positions. Thus the motion of the electrons is determined by where the nuclei are but not by how fast the nuclei are moving.

For a given distance between the nuclei it is possible to determine the energy, the wave function and the electron density distribution of the electrons, the nuclei being held in fixed positions. Then the distance between the nuclei is changed to a new value, and the calculation of the energy, wave function and electron density distribution of the electrons is performed again. This process, repeated for every possible internuclear distance, allows understanding of how the energy of the electrons changes as the distance between the nuclei is changed. However, for the purpose on this analysis only the motion of the electrons and hold the nuclei stationary at some particular value for the internuclear distance R, could be considered.

The energy of the electrons in a molecule is quantised, as it is in atoms. When the nuclei are held stationary at some fixed value of *R*, there are a number of allowed energy levels for the electrons. There are, however, no simple expressions for the energy levels of a molecule in terms of a set of quantum numbers, such as was the case with the hydrogen atom. As in the case of atoms, there is a wave function that governs the motion of all the electrons for each of the allowed energy levels. Each wave function again determines the manner in which the electronic charge is distributed in three-dimensional space.

7.1 An Electrostatic Interpretation of the Chemical Bond

In the light of the above discussion of a molecular electron density distribution, a molecule may be regarded as two or more nuclei imbedded in a rigid three-dimensional distribution of negative charge. There is a theorem of quantum mechanics that states that the force acting on a nucleus in a molecule may be determined by the methods of classical electrostatics. The nuclei in a molecule repel one another, since they are of like charge. This repulsive force, if unbalanced, would push the nuclei apart and the molecule would separate into atoms. In a stable molecule, however, an attractive force exerted by the negatively charged electron density distribution balances the nuclear force of repulsion. The usefulness of this approach lies in the fact that the stability of molecules in terms of the classical concept of a balance between the electrostatic forces of attraction and repulsion could be considered.

A chemical bond is thus the result of the accumulation of negative charge density in the region between the nuclei to an extent sufficient to balance the nuclear forces of repulsion. [2] This corresponds to a state of electrostatic equilibrium, as the net force acting on each nucleus, is zero for this one particular value of the internuclear distance. If the distance between the nuclei is increased from the equilibrium value, the nuclear force of repulsion is decreased. At the same time the force of attraction exerted by the electron density distribution is increased as the binding region is increased in size. Thus, when the radial distance is increased from its equilibrium value there are net forces of attraction acting on the nuclei which pull the two nuclei together again. A definite force would have to be applied to overcome the force of attraction exerted by the electron density distribution and separate the molecule into atoms. Similarly, if the value of radial distance is decreased from its equilibrium value, the force of nuclear repulsion is increased over its equilibrium value. At the same time, the attractive force exerted by the electron density is decreased, because the binding region is decreased in size. In this case there is a net force of repulsion pushing the two nuclei apart and back to their equilibrium separation. There is thus one value of radial distance for which the forces on the nuclei are zero and the whole molecule is in a state of electrostatic equilibrium. [2]

This is an important result as it shows that the density distribution in a molecule cannot be considered as the simple sum of the two atomic charge densities. The overlap of rigid atomic densities does not place sufficient charge density in the binding region to overcome the nuclear force of repulsion. Hence it is reasonable to conclude that the original atomic charge distributions

must be distorted in the formation of a molecule, and the distortion is such that charge density is concentrated in the binding region between the nuclei. A quantum mechanical calculation predicts this very result. The calculation shows that there is a continuous distortion of the original atomic density distributions, a distortion that increases as the internuclear distance decreases.

The changes in the original atomic density distributions caused by the formation of the chemical bond may be isolated and studied directly by the construction of a density difference distribution. Such a distribution is obtained by subtracting the density obtained from the overlap of the undistorted atomic densities separated by a radial distance, from the molecular charge distribution evaluated at the same value. Wherever this density difference is positive in value it means that the electron density in the molecule is greater than that obtained from the simple overlap of the original atomic densities. Where the density difference is negative, it means that there is less density at this point in space in the molecule than in the distribution obtained from the overlap of the original atomic distributions. Such a density difference map thus provides a detailed picture of the net reorganisation of the charge density of the separated atoms accompanying the formation of a molecule. This just proves that the density distribution resulting from the overlap of the undistorted atomic densities does not place sufficient charge density in the binding region to balance the forces of nuclear repulsion. The regions of charge increase in the density difference maps are, therefore, the regions to which charge is transferred relative to the separated atoms to obtain a state of electrostatic equilibrium and hence a chemical bond. From this point of view a density difference map provides a picture of the "bond density."

7.2 The Effect of the Pauli Principle on Chemical Binding

The Pauli exclusion principle plays as important a role in the understanding of the electronic structure of molecules as it does in the case of atoms. The end result of the Pauli principle is to limit the amount of electronic charge density that can be placed at any one point in space. For example, the Pauli principle prevents the 1*s* orbital in an atom from containing more than two electrons. Since the 1*s* orbital places most of its charge density in regions close to the nucleus, the Pauli principle, by limiting the occupation of the 1*s* orbital, limits the amount of density close to the nucleus. Any remaining electrons must be placed in orbitals that concentrate their charge density further from the nucleus. [2]

It is proven that the reason the electron doesn't fall onto the nucleus is because it must possess kinetic energy if Heisenberg's uncertainty principle is not to be violated. This is one reason why matter doesn't collapse. The Pauli principle is equally important in this regard. The electron density of the outer electrons in an atom cannot collapse and move closer to the nucleus since it can do so only if the electrons occupy an orbital with a lower n value. If, however, the inner orbital contains two electrons, then the Pauli principle states that the collapse cannot occur. The Pauli principle demands that when two electrons are placed in the same orbital their spins must be paired. What restriction is placed on the spins of the electrons during the formation of a molecule, when two orbitals, each on a different atom, overlap one another? To address this question a hydrogen molecule that consists of two hydrogen atoms is considered, where atom A has the configuration $1s^1$ and atom B has the configuration $1s^1$. Even when the atoms approach very close to one another the Pauli principle would be satisfied as the spins of the two electrons are opposed. This is the situation that has been assumed in all discussions of the hydrogen molecule.

However, what would occur if two hydrogen atoms approached one another and both had the same configuration and spin, say $1s^1$? When two atoms are relatively close together the electrons become indistinguishable. It is no longer possible to say which electron is associated with which atom as both electrons move in the vicinity of both nuclei. Indeed this is the effect which gives rise to the chemical bond. In so far as the region around each atom to be governed by its own

atomic orbital can be considered, distorted as it may be, two electrons with the same spin are not be able to concentrate their density in the binding region. This region is common to the orbitals on both atoms, and since the electrons possess the same spin they cannot both be there simultaneously. In the region of greatest overlap of the orbitals, the binding region, the presence of one electron tends to exclude the presence of the other if their spins are parallel. Hence, instead of density accumulating in the binding region as two atoms approach, electron density is removed from this region and placed in the antibinding region behind each nucleus where the overlap of the orbitals is much smaller. Thus, the approach of two hydrogen atoms with parallel spins does not result in the formation of a stable molecule. This repulsive state of the hydrogen molecule, in which both electrons have the same spin and atomic orbital quantum numbers, can be detected spectroscopically. [2]

Consequently, the general requirements for the formation of a chemical bond can be formulated. Electron density must be accumulated in the region between the nuclei to an extent greater than that obtained by allowing the original atomic density distributions to overlap. In general, the increase in charge density necessary to balance the nuclear force of repulsion requires the presence of two electrons.

In the atomic orbital approximation we picture the bond as resulting from the overlap of two distorted atomic orbitals, one centred on each nucleus. When the orbitals overlap, both electrons may move in the field of either nuclear charge as the electrons may now exchange orbitals. Finally, the pair of electrons must possess opposed spins. When their spins are parallel, the charge density from each electron is accumulated in the antibinding rather than in the binding region.

7.3 Classification of Chemical Bonds

To make a quantitative assessment of the type of binding present in a particular molecule it is necessary to have a measure of the extent of charge transfer present in the molecule relative to the charge distributions of the separated atoms. This information is contained in the density difference or bond density distribution, the distribution obtained by subtracting the atomic densities from the molecular charge distribution. Such a distribution provides a detailed measure of the net reorganisation of the charge densities of the separated atoms accompanying the formation of the molecule.

The density distribution resulting from the overlap of the undistorted atomic densities (the distribution which is subtracted from the molecular distribution) does not place sufficient charge density in the binding region to balance the nuclear forces of repulsion. The regions of charge increase in a bond density map are, therefore, the regions to which charge is transferred relative to the separated atoms to obtain a state of electrostatic equilibrium and hence a chemical bond. Thus, it is possible to use the location of this charge increase relative to the positions of the nuclei to characterise the bond and to obtain an explanation for its electrostatic stability.

A bond is classified as covalent when the bond density distribution indicates that the charge increase responsible for the binding of the nuclei is shared by both nuclei. It is not necessary for covalent binding that the density increase in the binding region be shared equally. It is possible to encounter molecules with different nuclei, in which the net force binding the nuclei is exerted by a density increase that, while shared, is not shared equally between the two nuclei. [2]

The charge distribution of a molecule with an ionic bond is characterised not only by the transfer of electronic charge from one atom to another, but also by a polarisation of each of the resulting ions in a direction counter to the transfer of charge. [2]

In a covalent bond the increase in charge density that binds both nuclei is shared between them, while in an ionic bond the forces exerted by the charge density localised on a single nucleus bind both nuclei. It must be stressed that there is no fundamental difference between the forces responsible for a covalent or an ionic bond, as they are electrostatic in both cases.

7.4 Interaction Between Molecules

The properties of matter observed on the macroscopic level are determined by the properties of the constituent molecules and the interactions between them. The polar or non-polar character of a molecule is clearly important in determining the nature of its interactions with other molecules. There are relatively strong forces of attraction acting between molecules with large dipole moments. To a first approximation, the energy of interaction between dipolar molecules can be considered as completely electrostatic in origin, the negative end of one molecule attracting the positive end of another.

The presence of intermolecular forces accounts for the existence of solids and liquids. A molecule in a condensed phase is in a region of low potential energy, as a result of the attractive forces that the neighbouring molecules exert on it. By supplying energy in the form of heat, a molecule in a solid or liquid phase can acquire sufficient kinetic energy to overcome the potential energy of attraction and escape into the vapour phase. The pressure of the vapour in equilibrium with a solid or liquid, at a given temperature, provides a measure of the tendency of a molecule in a condensed phase to escape into the vapour (the larger the vapour pressure, the greater the escaping tendency). The average kinetic energy of the molecule in the vapour is directly proportional to the absolute temperature. Thus the observation of a large vapour pressure at a low temperature implies that relatively little kinetic energy is required to overcome the potential interactions between the molecules in the condensed phase.

7.5 Polyatomic Molecules

The concept of a molecular orbital is readily extended to provide a description of the electronic structure of a polyatomic molecule. Indeed molecular orbital theory forms the basis for most of the quantitative theoretical investigations of the properties of large molecules.

In general a molecular orbital in a polyatomic system extends over all the nuclei in a molecule are essential, if the spatial properties of the orbitals are to be understood and predicted. An analysis of the molecular orbitals for the water molecule provides a good introduction to the way in which the symmetry of a molecule determines the forms of the molecular orbitals in a polyatomic system.

8. Conclusion

The main objective of this paper was to present Mirce Mechanics approach to Reliability, one that is based on the laws of science. This approach is in direct agreement with the observed with occurrence of negative functionability phenomena resulting from physical processes like corrosion, fatigue, creep, wear and similar.

Finally, it is essential to distinguish the scientific formulation of the motion of functionability through the life of a system, contained in Mirce Mechanics and presented in this paper, from the best "industrial practices" approach that is based on reliability models of systems that are created to demonstrate the contractual compliance of the legally binding acquisition processes. As science is the proved model of reality that is confirmed through observation, the summary message of this paper to reliability professionals is to move from the universe in which the laws of science are suspended to the universe that is based on the laws of science that govern behaviour of atoms in molecules of the matter, in order for their predictions to become future realities.

Acknowledgment

I wish with this paper to pass my very best wishes to Richard Bader, Emeritus Professor of McMaster University in Canada, for his 80th birthday. He revolutionised chemistry by introducing quantum mechanical approach its physical understanding that lead to the creation of the atoms in molecules theory [6]. Most material in this paper is based on the knowledge that Richard has accumulated during an extremely successful career and which he shared so enthusiastically with all of those who were able to embrace it.

References

1. Knezevic J., Reliability, Maintainability and Supportability – A Probabilistic Approach, with Probchar Software. pp. 292, McGraw Hill, UK, 1993.
2. Bader, R.F.W., An Introduction to the Electronic Structure of Atoms and Molecules, pp 240, Clark Irvin, 1970.
3. Knezevic, J., Physical Scale of Mirce Mechanics, Lecture Notice, Master Diploma Programme, MIRCE Akademy, Woodbury Park, Exeter, UK, 2009.
4. Knezevic, J., Functionability in Motion, Proceedings 10th International Conference on Dependability and Quality, DQM Institute, 2010, Belgrade, Serbia.
5. Knezevic, J., Scientific Scale of Reliability, Proceedings of International Conference on Reliability, Safety and Hazard, Bhabha Atomic Research Centre, 2010, Mumbai, India.
6. Bader, R.F.W., Atoms in Molecules: a Quantum Theory, Oxford University Press, Oxford, UK, 1990.

Life Cycle Reliability and Safety Engineering
Vol.1 Issue 1 (2012) 26-34

A Condition-Based Inspection-Maintenance Model Based on Geometric Sequences for Systems With a Degradation Process and Random Shocks

Wenjian Li and Hoang Pham
Rutgers University, USA

Abstract

In this paper we present a condition-based inspection-maintenance model for the systems subject to a degradation process and random shocks based on a geometric approach where the inter-inspection times are non-increasing. Upon the inspection of the system and its condition, inspectors need to decide whether to take an action such as preventive maintenance (PM) or corrective maintenance (CM), or no action is needed. We first derive an expected maintenance cost rate function subject to a degradation process and cumulative shock damage. Then we use the mean time to first failure as an initial solution approach to obtain the optimal maintenance policy consisting of two decision variables that minimizes the expected long-run maintenance cost per unit time. The two decision variables are the preventive maintenance threshold value and inspection times based on a geometric sequence. A numerical example is given to illustrate the optimal maintenance policy of the expected long-run cost rate model.

Keywords- *Condition-based maintenance, cumulative random shock damage, maintenance optimization, preventive maintenance, expected long-run cost rate, degradation process, geometric inspection sequence*

1. Introduction

Suppose that the state of a system can only be revealed through the inspection. This research we study an optimal inspection-maintenance strategy for repairable systems subject to degradation and random shocks. Grall et al [1] study the inspection-maintenance strategy for a single unit deteriorating system. The degradation is expressed by the Gamma process which implies the stationary and independent increment property. The maintenance cost function is developed based on regenerative and semi-regenerative process. Preventive and inspection schedule are two decision variables. While, in this research, it is assumed that the degradation and shock damage are measurable, otherwise there are some parameters associated with the processes which can be traced. The maintenance decision is made on the amount of degradation and shock damage which are measured, not on something abstract such as the distribution parameters or transition probability.

Grall, Berenguer and Dieulle [2] consider a system subject to a random deterioration process. They develop a model that allow to investigate the joint influence of the preventive maintenance threshold and inspection dates based on the average long-run cost rate assuming that the degradation process is a stationary law. In this research, we do not assume the stationary degradation process but the degradation follows the degradation paths and hope that, it is more practical. Pham et. al. [21] present a degradation model for predicting the reliability of k-out-of-n systems based on a Markov approach in which components are subject to multi-stage degradation and catastrophic failures. The same authors [22] later study models for predicting the availability and mean lifetime of multi-stage degraded systems with partial repairs. They, however, have not considered the maintenance aspects in their studies. Wang and Pham [23] recently develop a dependent competing risk model for systems subject to multiple degradation processes and random shocks using time-varying copulas. Their model considers a flexible dependence relationship between random shocks and degradation processes as well as the dependent relationship among various degradation processes.

So [6] studies the control limit policies for a multistate deteriorating system which is modeled by a semi-Markov process with a state space $\{0,\ldots,M\}$. A control limit policy is a policy such that when the system condition is worse than a certain threshold n

, a $_n$ $(1 \le n < M)$ restoration is initiated. Chelbi and Ait-Kadi [3] address the optimal inspection strategies for deteriorating equipments. They consider both preventive and corrective maintenance policies. If the value of the degradation process exceeds the alarm value, then preventive maintenance will be taken; if the system fails, a corrective maintenance will be performed. In their research, the inspection time x_i is a decision variable which is determined with a conditional probability p_i where p_i is defined as the probability that the alarm threshold is exceeded within the time interval $[x_{i-1}, x_i]$ given that such situation is not yet found at the inspection time x_{i-1}. Wang and Pham [15] recently study a multi-objective maintenance optimization embedded within the imperfect PM for a single-unit system with dependent competing risks of degradation wear and random shocks. They consider two kinds of random shocks in the system such as fatal shocks that will cause the system to fail immediately, and nonfatal shocks that will increase the system degradation level by a certain cumulative shock amount. In this research, we consider the two competing processes and then derive the expected maintenance cost rate based on the degradation paths instead of the conditional probability p_i. Markov process [4,8,24], semi-Markov process [11], and the stationary degradation process [1,2] have been commonly used to develop models for the systems subject to degradation.

In this research, we consider the two different degradation functions that describe degradation paths such as: (1) $Y(t) = A + Bg(t)$, where A and B are both random variables and are independent and $g(t)$ is a function of time t; (2) $Y(t) = \frac{e^{Bt}}{A + e^{Bt}}$ where A and B are two independent random variables. For the shock process, it is modeled by $D(t) = \sum_{i=0}^{N(t)} X_i$ where $X_i^{'}s$ are independent and identically distributed (i.i.d.) and $N(t)$ is a random variable follows a Poisson process, i.e., $N(t) \sim Poisson(\lambda)$ We also assume that the degradation $Y(t)$ and random shock $D(t)$ are independent. Let T denote the time-to-failure and is defined as , $T = \inf\{t > 0 : Y(t) > G \; or \; D(t) > S\}$ where G is the critical value for degradation and S is the threshold level for $D(t)$. Therefore, T is defined in terms of G and S.

Generally, maintenance is classified into condition-based or time-based. For the former, the action taken depends on the state of the system detected after each inspection, which could be determined to perform a PM, CM or nothing. For the CM, the maintenance action is performed at predetermined time intervals to bring the system to an improved working condition and would prefer as the condition-based maintenance. In this research, two maintenance actions are considered: preventive and corrective maintenance. The system is instantaneously inspected by time $I_1,\ldots,I_n$. At inspection time I_n, one of the two decisions has to be made:

(1) Determine whether the maintenance action is PM, CM, or the system as is, and

(2) Determine the time to next inspection.

In other words,

(i) When the state of a system revealed by an inspection is as , $Y(t) \le L \bigcap D(t) \le S$ the system is left as it is since the system is at very health condition.

(ii) When the system state upon the inspection is found as $L < Y(t) \le G \bigcap D(t) \le S$, the functioning system is considered as worn-out and a PM is triggered.

When the system fails caused by either degradation or random shocks, a CM is taken to restore the system to as good as new. PM is an active action to avoid the failure of a system during the actual operation since the cost and /or damage when the system failure is often large. L is called PM threshold level which is a control limit value. When the system state deteriorates to or beyond L, the system is preventively maintained.

It is assumed that no continuous monitoring is performed on the system. So the state of the system is only revealed after each inspection. The choice of the inspection times $\{I_1,..., I_i,...\}$ and PM threshold level L have great influence on the maintenance cost rate. L effectively divides the system state into two sets. On the one hand, a low L values will result in a frequently PM action and prevents the full usage of the residual life of the systems. Frequent PMs might reduce the chances of high deterioration and failures but it also costly. On the other hand, a high L values will keep the system working in a high risk

condition. For the condition-based maintenance, the regular inspection (equal inter-inspection) is more convenient to schedule. Although the losses due to down time can be reduced by frequent inspections, it might not always worthwhile to inspect the unit, especial if the inspection is expensive. Sequential inspection is more realistic. Li and Pham [20] recently discuss a condition-based maintenance modeling aspect in which the system is periodically inspected at an increasing equally time of intervals such as I, 2I, 3I,…nI where I is the first inspection time interval. A reason for such approach is that in some applications today, the preventive maintenance threshold is likely to be set conservatively and the inspection schedule may be performed more than necessary.

In reality, on the other hand, because of the aging effect, accumulated degradation, and shock damages, many systems are degenerative in the sense that the successive inspection time interval will be shorter and shorter. In other words, the inter-inspection times are decreasing. In this research, we consider such situation where a geometric sequence approach is applied. The inspection times sequence $\{I_1,..., I_i,...\}$ and a PM threshold level L are two important factors to be considered as decision variables for minimizing the expected long-run average cost rate. We develop a condition-based maintenance model for selecting the optimal inspection schedule and the PM threshold L for a single-unit system in order to balance the cost among PM, CM, inspection and losses due to idle time. In section 2, we describe the model assumptions and the inspection-maintenance policy. Sections 3 and 4 present a mathematical formulation for the cost rate model and the model optimization, respectively. Section 5 provides numerical examples to illustrate the results and finally conclude in section 6.

Notation

$Y(t)$	Degradation value
$D(t)$	Cumulative shock damage value up to time t
G	A critical value for degradation process
S	A critical value for shock damage
C_i	Cost per inspection
C_c	Cost per CM action
C_p	Cost per PM action
C_m	Loss per unit idle time
$C(t)$	Cumulative maintenance cost up to time t
$E[C_1]$	Average total maintenance cost during a cycle
$E[W_1]$	Mean cycle length
$EC(I_1,L)$	Expected long-run cost rate function
L	PM critical value
$E[N_I]$	Mean inspection number during a cycle
$N_p(t)$	Number of PM actions up to time t
$N_c(t)$	Number of CM actions up to time t
$N_I(t)$	Number of inspection in $(0,t]$
$\xi(t)$	Cumulative idle times in $(0,t]$
$E[\xi]$	Mean idle time during a cycle
$\{I_i\}_{i\in N}$	Inspection sequence
$\{U_i\}_{i\in N}$	Inter-inspection sequence
$\{W_i\}_{i\in N}$	Renewal times, W_1 first renewal time
T	Time to failure
P_{i+1}	Probability that there are total $i+1$ inspections in a renewal cycle

P_p Probability that a renewal cycle ends by a PM action

P_c Probability that a renewal cycle ends by a CM action

2. Model Description and Assumptions

2.1 Assumptions

The system starts at a new condition. The assumptions are as follows:

1. The system is not continuously monitored, but its can be detected only by inspection. Inspections are assumed instantaneous, perfect and non-destructive.
2. The system failure is only detected by inspection. Therefore, if the system fails, it remains failed until the next inspection which causes a loss of C_m per unit time. The system is then correctively replaced.
3. PM or CM will restore the system state to a as-good-as-new state.
4. As to the cost parameters, it is assumed that corrective maintenance is more costly than a PM. And, a PM costs much more than an inspection. That implies $C_c > C_p > C_i$.
5. Y(t) and D(t) are two random variables and are independent.

2.2. Inspection -Maintenance Policy

In this research, the system is proposed to be inspected at times I_1, I_2,…In. As the system ages, the more frequent inspection is needed. Hence, inspection intervals between two successive inspections become shorter and shorter. A geometric sequence is suitable for such situation. Therefore, the inspection sequence can be constructed as $I_n = \sum_{j=1}^{n} \alpha^{j-1} I_1$, where $0 < \alpha < 1$ and I_1 is the first inspection time. The inter-inspection interval can be written as $U_n = I_n - I_{n-1} = \alpha^{n-1} I_1$ where $\{U_i\}_{i \in N}$ is a decreasing geometric sequence.

According to the state detected at each inspection epoch, one has to take one of the following actions:

(1) If, $Y(I_i) \le L \; and \; D(I_i) \le S$ since the system is still at a good condition, we do nothing but determine the time to next inspection: $I_{n+1} = I_n + U_n$, i=1,….where U_n is inter-inspection time between n^{th} and $n+1^{th}$ and inspection.

(2) If $L < Y(I_i) \le G \; and \; D(I_i) \le S$, or the system is in a PM state and a PM is triggered. In other words, the system is not failed but already exceeded the PM threshold, a PM is performed.

(3) If $Y(I_i) \le L \cap D(I_i) > S$ $Y(I_i) > G \cap D(I_i) \le S$ $L < Y(I_i) \le G \cap D(I_i) > S$ or $Y(I_i) > G \cap D(I_i) > S$ the system is in a CM state, a CM is triggered. In other words, if the inspection reveals that the system has failed; then, a CM action is performed on the system.

It should be noted that the inspection sequence $\{I_1,..., I_i,...\}$ is a function of I_1 and α where α is given. Therefore, an interesting optimization decision-making problem here is to determine I_1 and L that minimizes the average long-run cost per unit time. After a PM or CM, the system renews. Obviously then a new sequence of inspections can begin which is defined in the same way.

3. Maintenance Cost Analysis

In this section, an explicit expression for the average long-run maintenance cost per unit time is derived which aims at optimizing the maintenance policy through finding both PM critical threshold value L and inspection sequence. Suppose that the time horizon is infinity. The total maintenance cost up to time t can be defined as:

$$C(t) = C_i N_I(t) + C_p N_p(t) + C_c N_c(t) + C_m \zeta(t) \quad (1)$$

According to the basic renewal theory, $\lim_{t\to\infty} \frac{C(t)}{t} = \frac{E[C_1]}{E[W_1]}$

Therefore, we will study the average total maintenance cost per unit time on a single renewal cycle instead of $\lim_{t\to\infty} \frac{C(t)}{t}$. We first need to derive the cost function $E[C_1]$.

The mean total maintenance cost during a cycle $E[C_1]$ can be expressed as:

$$E[C_1] = C_i E[N_I] + C_p P_p + C_c P_c + C_m E[\zeta] \quad (2)$$

where C_i represents the cost associated with each inspection; C_P represents each PM cost; C_c represents the CM cost (since failure is only found through inspection, if it occurs at instant T within the inspection time interval $[I_i, I_{i+1}]$, the system will remain idle during the interval $[T, I_{i+1}]$ and C_m is the penalty cost per unit time associated with such event.

In the following, we will perform the analytical analysis of the components in $E[C_1]$

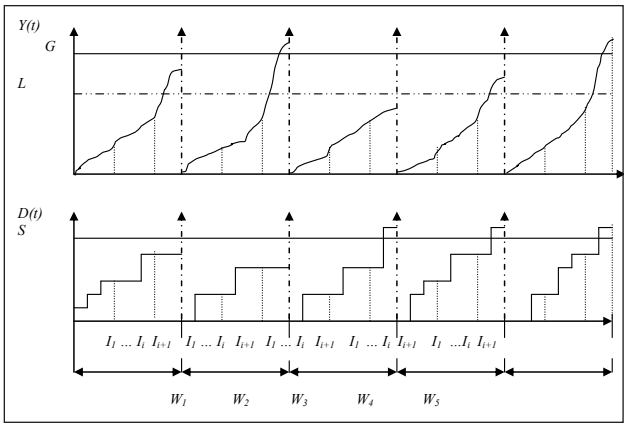

Fig. 1 : The diagram of the possible renewal cycle

1) Let $E[N_1]$ denote the mean inspection times during a cycle. $E[N_1]$ can be obtained as:

$$E[N_I] = \sum_{i=0}^{\infty} (i+1) P\{N_I = i+1\} \quad (3)$$

There will be a total of (i+1) inspections during a cycle if the first time to trigger a PM or CM action within the time interval $(I_i, I_{i+1}]$. In other word, the inspection will stop when the current inspection

finds that a PM or CM condition satisfied while this situation is not revealed in the previous inspection. Let $P\{N_1=i+1\}$ be the probability that a total of $(i+1)$ inspections occurred in one cycle. Therefore,

$$P_{i+1} = P\{N_1 = i+1\} = \bigcup_{j=1}^{5} P\{E_j\}$$

where

$$E_1 = Y(I_i) \le L, D(I_i) \le S \bigcap L < Y(I_{i+1}) \le G, D(I_{i+1}) \le S,$$

$$E_2 = Y(I_i) \le L, D(I_i) \le S \bigcap Y(I_{i+1}) > G, D(I_{i+1}) \le S,$$

$$E_3 = Y(I_i) \le L, D(I_i) \le S \bigcap Y(I_{i+1}) \le L, D(I_{i+1}) > S,$$

$$E_4 = Y(I_i) \le L, D(I_i) \le S \bigcap L < Y(I_{i+1}) \le G, D(I_{i+1}) > S,$$

$$E_5 = Y(I_i) \le L, D(I_i) \le S \bigcap Y(I_{i+1}) > G, D(I_{i+1}) > S.$$

The renewal cycle ends in 5 possible ways as shown in Figure 1. Defineas the probability that a cycle ends by i^{th} $(i=1,\ldots5)$ possibility at time I_{i+1} .

There is one more event $E_6 = (Y(I_i) \le L, D(I_i) \le S \bigcap Y(I_{i+1}) \le L, D(I_{i+1}) \le S)$ in the time interval $(I_i, I_{i+1}]$ which represents the functioning state of the system. That is

$$P\left\{\bigcup_{j=1}^{6} E_j\right\} = P\{Y(I_i) \le L, D(I_i) \le S\}$$

Therefore,

$$P_{i+1} = P\{\bigcup_{j=1}^{5} E_j\}$$

$$= P\{Y(I_i) \le L, D(I_i) \le S\} - P\{Y(I_{i+1}) \le L, D(I_{i+1}) \le S\} \quad (4)$$

2) Since a PM or CM action appears only once during a cycle, either of them will end a renewal cycle. As a consequence, $P_p+P_c=1$. In other words, both PM and CM events are mutually exclusive at a renewal time point. P_p is defined as:

$$P_p = P\{a\ PM\ action\ ends\ cycle \mid cycle\ is\ over\}$$

$$= \sum_{i=0}^{\infty} P\{a\ PM\ action\ ends\ cycle, N_1 = i+1 \mid cycle\ is\ over\}$$

$$= \sum_{i=0}^{\infty} P_{i+1}(E_1) \quad (5)$$

where .

$$P_{i+1}(E_1) = P\{Y(I_i) \le L, L < Y(I_{i+1}) \le G\} P\{D(I_{i+1}) \le S\}$$

Since PM and CM are mutually disjointed at renewal time, $P_c=1-P_p$.

To compute , $P\{Y(I_i) \le L, L<Y(I_i) \le G\}$ while $Y(I_i)$ are $Y(I_{i+1})$ dependent, we need to obtain the joint p.d.f $f_{Y(I_i),Y(I_{i+1})}(x_1,x_2)$ of $Y(I_i)$ and $Y(I_{i+1})$. of. We now explore the following two different degradation functions for $Y(t)$:

(1) Assume $Y(t)=A+Bg(t)$ where A and B are independent. Assume that $A \sim f_A(a),\ B \sim f_B(b)$.

Let $\begin{cases} y_1 = a + bg(I_i) \\ y_2 = a + bg(I_{i+1}) \end{cases}$

After solving the above equations in terms of y_1 and y_2 , we have:

$$a = \frac{y_1 g(I_{i+1}) - y_2 g(I_i)}{g(I_{i+1}) - g(I_i)} = h_1(y_1, y_2)$$

$$b = \frac{y_2 - y_1}{g(I_{i+1}) - g(I_i)} = h_2(y_1, y_2)$$

Suppose $y_1, y_2, h_1(y_1,y_2)$, and $h_2(y_1,y_2)$ are continuous and the partial derivatives $\frac{\partial h_1}{\partial y_1}, \frac{\partial h_1}{\partial y_2}, \frac{\partial h_2}{\partial y_1}$ and $\frac{\partial h_2}{\partial y_2}$ are differentiable. Then the Jacobian J is given by .

$$J = \begin{vmatrix} \frac{\partial h_1}{\partial y_1} & \frac{\partial h_1}{\partial y_2} \\ \frac{\partial h_2}{\partial y_1} & \frac{\partial h_2}{\partial y_2} \end{vmatrix} = \left| \frac{1}{g(I_i) - g(I_{i+1})} \right|.$$

Then the random vector $(Y(I_i), Y(I_{i+1}))$ has a joint continuous probability density function (pdf) given by:

$$f_{Y(I_i),Y(I_{i+1})}(y_1,y_2) = |J| f_A(h_1(y_1,y_2)) f_B(h_2(y_1,y_2)) \quad (6)$$

(2) Assume $Y(t) = \frac{e^{At}}{B + e^{At}}$ where A and B are independent.

Assume $A \sim f_A(a),\ B \sim f_B(b)$.

Let $\begin{cases} y_1 = \frac{e^{at}}{b + e^{at}} \\ y_2 = \frac{e^{at}}{b + e^{at}} \end{cases}$

The above equations can be uniquely solved for a and b in terms of y_1 and y_2 with solutions given by

$$\begin{cases} a = \dfrac{\ln\left(\dfrac{y_2(y_1-1)}{y_1(y_2-1)}\right)}{I_{i+1}-I_i} = h_1(y_1,y_2) \\ b = -\dfrac{e^{\frac{\ln\left(\frac{y_2(y_1-1)}{y_1(y_2-1)}\right)I_{i+1}}{I_{i+1}-I_i}}(y_2-1)}{y_2} = h_2(y_1,y_2) \end{cases}$$

Suppose that the functions $h_1(y_1, y_2)$ and $h_2(y_1, y_2)$ have continuous partial derivatives. The following is a 2x2 Jacobian determinant:

$$J = \frac{y_1(y_2-1)\left(\frac{y_2}{y_1(y_2-1)} - \frac{y_2(y_1-1)}{y_1^2(y_2-1)}\right)\left(-d(y_1,y_2) - d_1(y_1,y_2) + d_2(y_1,y_2)\right)}{y_2(y_1-1)(I_{i+1}-I_i)} + d_3(y_1,y_2)$$

Where

$$d(y_1,y_2) = \frac{\left(\left(\frac{y_1-1}{y_1(y_2-1)} - \frac{y_2(y_1-1)}{y_1(y_2-1)^2}\right) y_1(y_2-1)^2 I_{i+1} e^{\left(\frac{\ln\left(\frac{y_2(y_1-1)}{y_1(y_2-1)}\right)I_{i+1}}{I_{i+1}-I_i}\right)}\right)}{y_2^2(y_1-1)(I_{i+1}-I_i)},$$

$$d_1(y_1,y_2) = \frac{e^{\left(\frac{\ln\left(\frac{y_2(y_1-1)}{y_1(y_2-1)}\right)I_{i+1}}{I_{i+1}-I_i}\right)}}{y_2}$$

$$d_2(y_1,y_2) = \frac{e^{\left(\frac{\ln\left(\frac{y_2(y_1-1)}{y_1(y_2-1)}\right)I_{i+1}}{I_{i+1}-I_i}\right)}(y_2-1)}{y_2^2},$$

$$d_{31}(y_1,y_2) = \left(\frac{y_1-1}{y_1(y_2-1)} - \frac{y_2(y_1-1)}{y_1(y_2-1)^2}\right) y_1^2(y_2-1)^3,$$

$$d_{32}(y_1,y_2) = \left(\frac{y_2}{y_1(y_2-1)} - \frac{y_2(y_1-1)}{y_1^2(y_2-1)}\right) I_{i+1} e^{\left(\frac{\ln\left(\frac{y_2(y_1-1)}{y_1(y_2-1)}\right)I_{i+1}}{I_{i+1}-I_i}\right)},$$

$$d_3(y_1,y_2) = \frac{d_{31}(y_1,y_2)d_{32}(y_1,y_2)}{y_2^3(y_1-1)^2(I_{i+1}-I_i)^2}.$$

It can be shown that the random vector $(Y(I_i), Y(I_{i+1}))$ are jointly continuous with a joint density function given by:

$$f_{Y(I_i),Y(I_{i+1})}(y_1,y_2) = |J| f_A(h_1(y_1,y_2)) f_B(h_2(y_1,y_2)) \quad (7)$$

For example, given $A \sim U[0,a]$ and $B \sim Weibull(\eta,\beta)$. The joint pdf is given by

$$f_{Y(I_i),Y(I_{i+1})}(y_1,y_2) = |J| \frac{1}{a}\frac{\beta}{\eta}\left(-\frac{e^{\frac{\ln\left(\frac{y_2(y_1-1)}{y_1(y_2-1)}\right)I_{i+1}}{I_{i+1}-I_i}}(y_2-1)}{y_2\eta}\right)^{\beta-1} e^{\left(-\frac{e^{\frac{\ln\left(\frac{y_2(y_1-1)}{y_1(y_2-1)}\right)I_{i+1}}{I_{i+1}-I_i}}(y_2-1)}{y_2\eta}\right)^{\beta}}, \quad (8)$$

If $0 < \dfrac{\ln\left(\dfrac{y_2(y_1-1)}{y_1(y_2-1)}\right)}{I_{i+1}-I_i} < a$.

In the above, we have paved the path how to compute. $P\{Y(I_i) \le L, L < Y(I_{i+1}) \le G\}$

3) When $I_i < T \le I_{i+1}$ the unit will be idle during the interval $[T, I_{i+1}]$. Let $E[\zeta]$ denote the average idle time between the failure occurrence epoch and its inspection during one cycle. $E[\zeta]$ is calculated as follows:

$$E[\zeta] = \sum_{i=0}^{\infty}\left(\bigcup_{j=2}^{5} P_{i+1}(E_j)\right)\int_{I_i}^{I_{i+1}}(I_{i+1}-t)f_T(t)dt$$

$$= \sum_{i=0}^{\infty} P\{Y(I_i) \le L, Y(I_{i+1}) > G\} P\{D(I_i) \le S\}\left(F(I_i)(I_i - I_{i+1}) + \int_{I_i}^{I_{i+1}} F(t)dt\right) \quad (9)$$

where $f_T(t) = \dfrac{d}{dt}(F(t))$, is the p.d.f of T and .

$$F(t) = P\{Y(t) \le G, D(t) > S\} + P\{Y(t) > G, D(t) \le S\}$$

Next we will need to obtain the expected cycle length function. The mean cycle length $E[W_1]$ is calculated as follows:

$$E[W_1] = E[E[W_1 \mid N_I]]$$

$$= \sum_{i=0}^{\infty} E[W_1 \mid N_I = i] P\{N_i = i\}$$

$$= \sum_{i=0}^{\infty} I_{i+1} P_{i+1} \quad (10)$$

EC is a function of inspection times $\{I_1,,,,I_i,,,,\}$ and PM threshold *L* through, P_p, P_c,$E[N_1]$, $E[\zeta]$ and $E[W_1]$. We then, in section 4, determine the optimal inspection sequence $\{I_1,.....,I_i,...\}$ and PM threshold level *L* which minimizes the long run average cost per unit time, *EC*.

4. Optimization Maintenance Policy

In section 3, we discuss each component of the expected long-run maintenance cost rate. In this section, we determine I_1 and *L* so that the expected long-run maintenance cost rate is minimized. The following optimization problem is formulated in terms of decision variables I_1 and *L* ($0<L \le G$)

$$\text{Min: } EC(I_1,L)=\frac{C_i\sum_{i=0}^{\infty}(i+1)\{P\{Y(I_i)\le L,D(I_i)\le S\}-P\{Y(I_{i+1})\le L,D(I_{i+1})\le S\}\}}{\sum_{i=0}^{\infty}I_{i+1}\{P\{Y(I_i)\le L,D(I_i)\le S\}-P\{Y(I_{i+1})\le L,D(I_{i+1})\le S\}\}}$$

$$+\frac{C_p\sum_{i=0}^{\infty}P\{Y(I_i)\le L,L<Y(I_{i+1})\le G\}P\{D(I_{i+1})\le S\}}{\sum_{i=0}^{\infty}I_{i+1}\{P\{Y(I_i)\le L,D(I_i)\le S\}-P\{Y(I_{i+1})\le L,D(I_{i+1})\le S\}\}}$$

$$+\frac{C_c\left\{1-\sum_{i=0}^{\infty}P\{Y(I_i)\le L,L<Y(I_{i+1})\le G\}P\{D(I_{i+1})\le S\}\right\}}{\sum_{i=0}^{\infty}I_{i+1}\{P\{Y(I_i)\le L,D(I_i)\le S\}-P\{Y(I_{i+1})\le L,D(I_{i+1})\le S\}\}}$$

$$+\frac{C_m\sum_{i=0}^{\infty}P\{Y(I_i)\le L,Y(I_{i+1})>G\}P\{D(I_i)\le S\}}{\sum_{i=0}^{\infty}I_{i+1}\{P\{Y(I_i)\le L,D(I_i)\le S\}-P\{Y(I_{i+1})\le L,D(I_{i+1})\le S\}\}} \quad (11)$$

It is difficult to obtain the closed-form expression for the optimal inspection-maintenance policy (I^*_1,L^*) that minimizes the equation (11). Since this is a two-dimension decision variable, one can use the *traditional optimization method* to obtain a local minimal optimum solution. General idea is to fix one dimension such as I_1 and search for a local minimal value *L* and so forth, given that one needs to provide the initial value for I_1. However, depend on the initial value of I_1, the local solution may still not closed enough to the optimum solution. To improve the search for obtaining a closed-best solution, we use the idea in [20] by considering the mean time to first failure as an initial solution for I_1 to begin with for searching the optimum solution. After several trials and numerous calculations compared between the traditional optimization method (that is, without the knowledge of the mean time to first failure calculation) and our proposed procedure, we observe that our approach converges quickly to the "best" local solution, if not global solution. Below is our proposed algorithm that uses to obtain the "best" local solution for the proposed model in equation (11).

Algorithm:

Step 1: Initialize the cost parameters C_i, C_p, C_c and C_i, Let initial $I_1=E[T]$, where

$$E[T]=\int_0^{\infty}P\{T>t\}dt=\int_0^{\infty}P\{Y(t)\le G,D(t)\le S\}dt \quad (12)$$

Step 2: Search one-dimensional minimal value along *L* direction and record it as $EC(I^*_1,L^*)$

Step 3: Increase I_1 value. Let $I_1 = I_1 + \Delta$ where Δ is a small increment.

Step 4: Search new one-dimensional minimal value along *L* direction and record it as $EC(I_1',L')$

Step 5: If $EC(I_1^*,L^*) > EC(I_1',L')EC(I_1^*,L^*) = EC(I_1',L')$ And, go to Step 3. If $EC(I_1^*,L^*)> EC(I_1',L')$, $EC(I_1^*,L^*)= EC(I_1',L')$ and go to Step 6.

Step 6: Stop.

5. Numerical Examples

For the degradation function $Y(t)=A+Bg(t)$ assuming $A\sim U[0,2]$, $B\sim Exp(-0.2)$ and $g(t) = te^{0.01t}$.For the random shock damage $D(t)=\sum_{i=1}^{N(t)}X_i$ assuming that $X_i\sim Exp(-0.04t)$ and $N(t)\sim Poisson(0.1)$. Given $G=50$, $S=100$, $a = 0.98$ and the cost parameters as: $C_i = 200$ per inspection, $C_c = 5600$ per CM, $C_p = 3000$ per PM, $C_m = 700$ per unit time.

The inspection sequence $\{I_1,.....,I_n,...\}$ is constructed using the formula $I_n=\sum_{j=1}^{n}\alpha^{j-1}I_1$, where $\alpha = 0.8$.We now determine both the value of $I_1$and *L* so that the expected total cost per unit time, $EC(I_1,L)$, is minimized. We first need to calculate the mean time to first failure and from equation (12), we obtain $E[T]$=40.8**.** Therefore, an initial value for I_1 is $I_1 = 40.8$

Figure 2 pictures a 3D long-run average total cost rate in terms of *L* and I_1. The optimum solutions for the PM threshold level and inspection sequence are $I_1 = 58$ and L=28, respectively, and the corresponding expected long-run cost rate is $EC(I_1,L) = 94.63$ where the average total maintenance cost during a cycle and the mean cycle length are, respectively, $E[C_1]$ =5685.13 and $E[W_1] = 60.07$. The optimal results balance the cost of inspections, preventive maintenance, corrective maintenance and penalty associated with idle time.

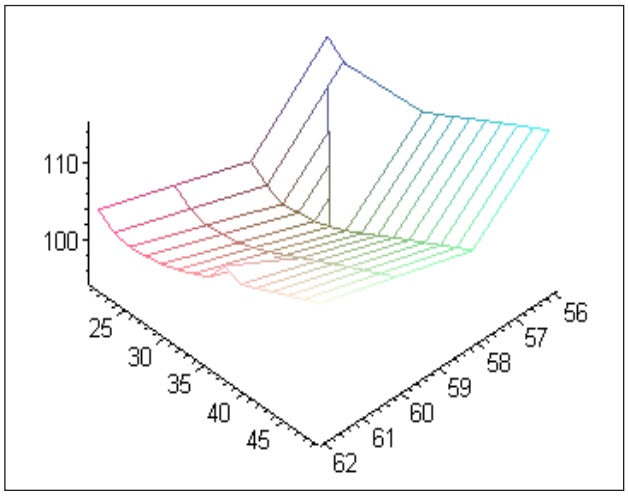

Fig.2. 3D Graph of EC(I1,L)

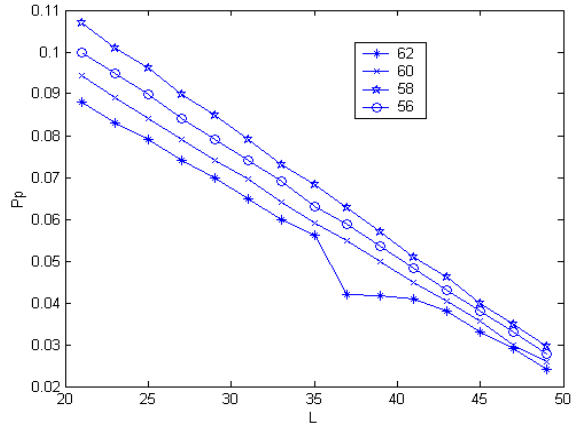

Figure 3. Pp *vs PM Threshold Value L*

Table I. P_{i+1} and Inspection Sequence

$P_1 = .9735$	$I_1 = 58$
$P_2 = .01922$	$I_2 = 114.84$
$P_3 = .0048$	$I_3 = 170.54$
$P_4 = .0016$	$I_4 = 225.13$
$P_5 = .000554$	$I_5 = 278.62$
$P_6 = .00076$	$I_6 = 331.05$

Table 1 lists the optimal inspection sequence and its probability P_{i+1}.

Figure 3 depicts the values of P_p vs PM threshold values of L for various values of I_1's such as I_1=62, I_1=60, I_1=58 and I_1=56

Note that this probability function

$$P\{Y(I_i) \le L, L < Y(I_{i+1}) \le G\} =$$

$$\int_L^G \int_{y_2 g(I_i)/g(I_{i+1})}^{(2(g(I_{i+1})-g(I_i))+y_2 g(I_i))/g(I_{i+1})} f_{Y(I_i),Y(I_{i+1})}(y_1, y_2)\, dy_1 dy_2$$

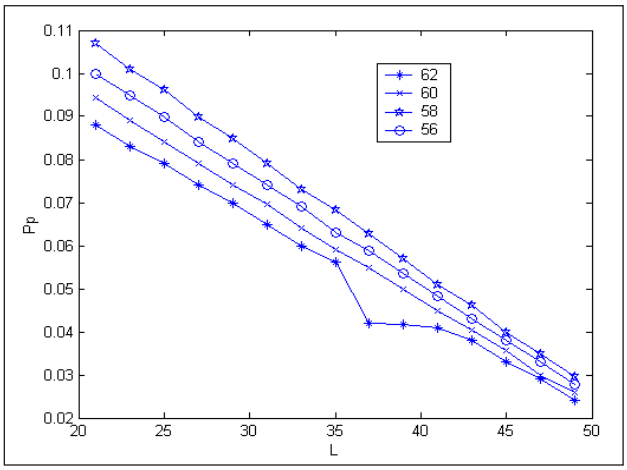

Figure 4. E[ζ]vs PM Critical Value LSYm

is a decreasing function of L as L increases. Therefore, it can be shown that

$$P_p = \sum_{i=0}^{\infty} P_{i+1}(E_1) = \sum_{i=0}^{\infty} P\{Y(I_i) \le L, L < Y(I_{i+1}) \le G\} P\{D(I_{i+1}) \le S\}$$

is also a decreasing function of L. Consequently, P_c increases as L increases since *Pc = 1-Pp* From the figure 3, we easily observe that, *Pp* is a decreasing function of *L*.

Figure 4 pictures the expected idle time during a cycle $E[\xi]$ versus the PM critical values of *L* for various inspection sequences such as: $I_1 = 62$, $I_1 = 60$, $I_1 = 58$ and $I_1 = 56$.

Since

$$P\{Y(I_i) \le L, Y(I_{i+1}) > G\} = \int_G^{\frac{Lg(I_{i+1})}{g(I_i)}} \int_{\frac{y_2 g(I_i)}{g(I_{i+1})}}^{\frac{(2(g(I_{i+1})-g(I_i))+y_2 g(I_i))}{g(I_{i+1})}} f_{Y(I_i),Y(I_{i+1})}(y_1, y_2)\, dy_1 dy_2$$

is an increasing function as L increases, it can be shown that the mean idle time during a cycle

$$E[\xi] = \sum_{i=0}^{\infty} P\{Y(I_i) \le L, Y(I_{i+1}) > G\} P\{D(I_i) \le S\} \int_{I_i}^{I_{i+1}} (I_{i+1} - t) f_T(t)\, dt$$

also increases as L increases. From the figure 4, we also observe that $E[\xi]$ is an increasing function of *L*.

6. Conclusion

This paper we present a condition-based inspection-maintenance model for degraded systems with respect to degradation process and random shocks

based on geometric sequences for inspection intervals. We determine the optimum decision variables for the PM threshold level L and the inspection sequence that minimizes the expected long-run cost rate. The difference between the proposed condition-based inspection/maintenance policy and a classical periodic inspection is that the periodic inspection times which constitutes a shorter and shorter inter-inspection sequence, instead of a larger inter-inspection sequence [20]. This sequence brings realistic implementations to several critical applications in practices using geometric sequence approach. The proposed policy is based on the measurable amount of the degradation and shock damage instead of assuming the processes modeled by Markov, semi-Markov process or imposing some constraints on the process in order to make the model computable. These advantages make our model practicable and interesting.

References

1. A. Grall, L. Dieulle, C. Berenguer and M. Roussignol, "Continuous-time predictive-maintenance scheduling for a deteriorating system", IEEE Trans. Reliability, Vol. 51, No. 2, pp 141-150, 2002
2. A. Grall, C. Berenguer and L. Dieulle, "A condition-based maintenance policy for stochastically deteriorating systems", Reliability Engineering and System Safety, vol. 76, pp 167-180, 2002
3. A. Chelbi and D. Ait-Kadi, "An optimal inspection strategy for randomly failing equipment", Reliability Engineering System Safety, vol. 63, pp 127-131, 1999
4. S. Bloch-Mercier, "A preventive maintenance policy with sequential checking procedure for a Markov deteriorating system", European Journal of Operational Research, Vol.147, pp 548-576, 2002
5. M. Ohnishi, H. Kawai and H. Mine, "An optimal inspection and replacement policy for a deteriorating system", Journal of Applied Probability. vol.23, pp 973-988, 1986
6. K.C. So, "Optimality of control limit policies in replacement models", Naval Research Logistics, vol.39, pp 685-697, 1992
7. M.M. Hosseini, R.M. Kerr and R.B. Randall, "An inspection model with minimal and major maintenance for a system with deterioration and Poisson Failures", IEEE Trans. on Reliability, vol. 49, no.1, pp 88-98, 2000
8. C.T. Lam, and R.H. Yeh, "Optimal maintenance-policies for deteriorating systems under various maintenance strategies", IEEE Trans. on Reliability, Vol.43, No.3, pp 423-430, 1994
9. C.T. Lam, and R.H. Yeh, "Optimal replancement policies for multistate deteriorating systems", Naval Research Logistics, vol. 41, pp 303-315, 1994
10. Sheu, S.H., "Extended optimal replacement model for deteriorating systems", European Journal of Operational Research, vol.112, pp 503-516, 1999
11. R.M. Feldman, "Optimal replacement with semi-Markov shock models",Journal of Applied Probability, vol.13, pp 108-117, 1976
12. C.T Chen, Y.W. Chen and J. Yuan, "On a dynamic preventive maintenance policy for a system under inspection", Reliability Engineering and System Safety, vol.80, pp 41-47, 2003
13. H.Z. Wang, "A survey of maintenance policies of deteriorating systems", European Journal of Operational Research, vol.139, pp 469-489, 2002
14. H.M. Taylor, "Optimal replacement under additive damage and other failure models", Naval Res. Log. Quart, Vol.22, pp 1-18, 1975
15. Y. Wang and H. Pham, "A multi-objective optimization of imperfect preventive maintenance policy for dependent competing risk systems with hidden failure", IEEE Trans. on Reliability, vol. 60, no.4, 2011 (in press)
16. Y. Lam, Y.L. Zhang and Y.H. Zheng, "A geometric process equivalent model for a multistate degenerative system", European Journal of Operational Research, vol. 142, pp 21-29, 2002
17. C.J. Lu and W. Q. Meeker, "Using degradation measures to estimate a time-to-failure distribution", Technometrics, vol. 35, no.2, May 1993, pp161-174
18. S.P. Wilson, "Failure modeling with multiple scales", George Washington University, Ph.D Dissertation, 1993
19. L. Dieulle, C. Berenguer, A. Gralland and M. Roussignol, "Sequential condition-based maintenance scheduling for a deteriorating system", European Journal of Operational Research, vol. 150, 451-461, 2003
20. W. Li and H. Pham, "A condition-based maintenance model for periodically inspected systems subjected to competing failure processes", International Journal of Systems Assurance Engineering and Management (in press)
21. H. Pham, A. Suprasad and R.B. Misra "Reliability and MTTF prediction of k-out-of-n complex systems with components subjected to multiple stages of degradation", International Journal of Systems Science, vol. 27, no. 10, pp. 995-1000,1996
22. H. Pham, A. Suprasad and R.B. Misra, "Availability and mean life time prediction of multistage degraded system with partial repairs", Reliability Engineering and System Safety Journal, vol. 56, pp. 169-173, 1997
23. Y. Wang and H. Pham, "Modeling the dependent competing risks with multiple degradation processes and random shock using time-varying copulas", IEEE Trans. on Reliability, vol. 60, no.4, December 2011 (in press)
24. M.J. Zuo, B. Liu and D.N.P Murthy, "Replacement-repair policy for multi-state deteriorating products under warranty", European Journal of Operational Research, vol. 123, pp 519-530, 2000